

## **Response to referees:**

# **Response of sub-ice platelet layer thickening rate to variations in Ice Shelf Water supercooling in McMurdo Sound, Antarctica**

5 Chen Cheng, Adrian Jenkins, Paul R. Holland, Zhaomin Wang, Chengyan Liu, and Ruibin Xia

10

*This response comprises Reply to Referee #1, Reply to Referee #2, and Reply to Ken Hughes. Each of our replies to the referees is structured as a sequence of comments from the referee, our response, and changes made to the manuscript.*

Note: *Italic* denotes the referees' comments, and the following is our response. "P\*L#" denotes line # in page \* of the 'tracked changes' version of the manuscript in which blue characters exactly represent the revised part. Double quote represents the excerpt of the revised manuscript. Almost all the references mentioned in this report can be found in the **References** section of the manuscript; otherwise, we have given the full citation.

## Reply to Referee #1:

### 1 General comments

5 The goal of the paper is to understand the relationship between supercooling, frazil concentration and platelet ice accumulation rate. The authors apply a model that some of them had published in JPO in 2017. The claimed novelty of this model is that it considers the vertical distribution of supercooling and frazil ice concentration. The model is applied to

McMurdo Sound and agrees with observations better than previous models. The authors try to understand the complex behaviour of the model through a (in some ways extensive) series of sensitivity experiments.

10 My overall evaluation is that the paper needs major revision before it could be published in *The Cryosphere*. I do think that the paper is interesting, timely, and that the idea of improving frazil ice models by considering variation with depth is worthwhile. However, I don't think the modelling performed is particularly novel and there are important limitations to the sensitivity experiments performed that limit the significance of the results. The explanations of the results (which are arguably the main interest for a general audience) are somewhat underdeveloped. I hope the authors are able to address the specific issues, which I discuss in detail below.

15

We thank the Referee #1 for his/her pertinent assessment of our paper and very constructive comments, which have helped us to improve our manuscript. We hope to address all the specific issues below.

### 2 Specific comments

20 1. The authors claim there are two differences in their model compared to previous studies. They consider: (1) the vertical distribution of supercooling; (2) the vertical distribution of frazil ice. I think that effect (1) is not really novel, despite the claim 'Cheng et al. (2017) introduced ... the linear depth-dependence of supercooling into [equation] (1)' (see page 4, line 2). As I understand, several previous studies that the authors reference considered this effect. For example, Smedsrud and Jenkins (2004) mention the 'depth-averaged freezing point used to calculate [the growth rate]' in paragraph 32. Jenkins and

25 Bombosch (1995) seem to say the same thing (around equation 15). I could certainly believe that this effect matters, but I don't think this paper can really claim to be novel in this respect, at least in the context of ISW plume models. The discussion in Cheng et al. (2017) seems to better reflect that effect (1) has been previously considered by various studies.

Indeed, previous studies have introduced the linear distribution of supercooling into equation 1 but with the assumption of

30 vertically-uniform frazil concentration, which leads to the adoption of supercooling at the mid-depth of Ice Shelf Water (ISW) plume. However, in this study, we didn't aim to emphasize the vertical distributions of supercooling and frazil concentration separately but their combined nonlinear effects: "A **vertically-modified** frazil-ice-laden ISW plume model that encapsulates the combined nonlinear effects of the vertical distributions of supercooling and frazil concentration..." (P1L14-15), "Here we first analyze the combined nonlinear effects of the vertical distributions of supercooling and frazil

35 concentration on..." (P3L6), "In this study, we demonstrated how the vertical distributions of supercooling and frazil ice

concentration within an ISW plume jointly determine the growth of suspended frazil ice,...” (P11L2-3). The complex behaviour shown in the results (which have been improved in the revised manuscript) of the sensitivity experiments do reflect these combined effects rather than their independent roles. The previous wording implied some misunderstanding of the novelty, so we have rewritten the sentences by deleting the phrases about the introduction of the vertical distribution of supercooling: “, Cheng et al. (2017) showed that adopting an approach in which the frazil ice growth is calculated using a vertically-uniform frazil concentration results in...” (P2L19-20), “In earlier ISW plume models, because  $c_i$  is treated as vertically-uniform, the integral of (1) can be represented by the product of the depth-averaged values  $T_{SC}^{0.5}$  (0.5 means at mid-depth) and  $C_i$ .” (P3L27-28), and “Accordingly, Cheng et al. (2017) introduced (2) into (1), ...” (P4L25).

10 *Effect (2) is novel in this context, although there are some studies in other contexts. For example, see Svensson and Omstedt (1998) in Cold Reg. Sci. Tech. The authors should reference and discuss this the introduction. However, I am not entirely persuaded that effect (2) is important in the context of this study. Naively, I would expect that the frazil rise velocity (say mm/s) is much smaller than the shear velocity, in which case the frazil ice concentration is almost vertically uniform in practice.*

15

We have added statements about the work of Svensson and Omstedt (1998) in Cold Reg. Sci. Tech. as well as Holland and Feltham (2005) in J. Fluid Mech. in the **Introduction**. That is, “Idealized one dimensional models confirm that the vertical distribution of frazil concentration cannot remain well-mixed in the upper layers of the ocean (Svensson and Omstedt, 1998) and beneath ice shelves (Holland and Feltham, 2005).” (P2L21-23). Again, we emphasize the combined effects of the vertical distributions of supercooling and frazil concentration in this study, and the results of the sensitivity runs serve to demonstrate its importance. The buoyant rise of the crystals must lead to some deviation from vertical uniformity, and we show the impact of that through the dependence of our results on the suspension index. Our standard run, which matches best with observation, has mean suspension index of 2.36, giving considerable variation in ice concentration over depth (Figure 2).

25

*2. More broadly, it seems there is the potential for inconsistency in modelling some quantities (such as the water temperature) as vertically uniform, while modelling the frazil ice concentration as varying with depth. Could the authors discuss this issue more clearly and add some justification*

30 It is a commonly used assumption in one- and two-dimensional depth-integrated ISW plume modeling that the water temperature and salinity within the plume are vertically uniform, and that assumption has some support in field observations, particularly those made in zones of freezing. Referring to this issue, we extended the previous sentences to “To date, all the ISW plume models mentioned above have been depth-integrated, and all the scalar quantities, i.e., water temperature, salinity, and frazil concentration in those models are treated as vertically-uniform. The well-mixed temperature and salinity

have been validated by borehole observations beneath the Amery Ice Shelf (Herraiz-Borreguero et al., 2013) and under the sea ice in McMurdo Sound (Robinson et al., 2014; HU14).” in P2L14-17.

3. I think the presentation of the model and the discussion of the results lost sight of the fact that frazil crystals grow by increasing in size.

We agree with the fact that frazil crystals grow by increasing in size naturally. In this study, we adopted a commonly used scheme proposed by Smedsrud and Jenkins (2004) to calculate the transfer processes, induced by frazil freezing and melting, between different size classes. To make this fact clearer, we added a statement “The frazil ice size distribution is represented by 5 crystal size classes, and the transfer processes, induced by frazil freezing and melting, between different size classes are calculated using the scheme proposed by Smedsrud and Jenkins (2004).” to the model description in P6L9-11.

*In section 2, it was not immediately clear that several quantities like  $c_i$  are a function of crystal size, although the authors do point out that crystal size determines the rise velocity.*

4. Equation (2) is somewhat hard to understand. Where does the factor 6 come from? It could be incorporated into  $Z^*$  in any case. An advection-diffusion equation in  $z$  needs two boundary conditions to determine the two integration constants. One comes from the vertical average  $C_i$  but what about the other. It looks like neither  $c_i$  nor its gradient are zero at  $\sigma = 0$ . Additionally, I think the factor of  $\sigma$  in the denominator is a typographic mistake.

[Reading Cheng et al. (2017), it seems that this the factor of 6 is an average inverse diffusivity based on some previous studies, but I think it is important that the present manuscript discusses equation (2) more fully, given that it is the main novel aspect of the paper.]

Thank you for the careful checking of the equations. As suggested, we have given a fuller presentation of the derivation of equation (2):

“ Considering only the balance between the buoyant-rise-induced vertical advection and turbulent diffusion terms, the governing equation for frazil concentration can be written as

$$\frac{d}{d\sigma} \frac{K}{D} \frac{dc_i}{d\sigma} + w_i \frac{dc_i}{d\sigma} = 0,$$

where  $w_i$  is the frazil ice rise velocity, determined by ice crystal size,  $K$  is the vertical frazil concentration diffusion coefficient, which can be parameterized as vertically constant (Cheng et al., 2013, 2016):

$$K = \frac{1}{6} \kappa u_* D,$$

where  $\kappa = 0.4$  is von Karman's constant,  $u_* = \sqrt{C_d}U$  is the friction velocity, related to the turbulent intensity within the ISW plume,  $C_d$  is the basal drag coefficient,  $U = \sqrt{(U_p + U_a)^2 + (V_p + V_a)^2 + U_t^2}$  is the total flow speed,  $U_p(U_a)$  and  $V_p(V_a)$  are the depth-averaged ISW plume (ambient current) speed in the  $x$  and  $y$  directions respectively,  $U_t$  is the root-mean square tidal speed. Using a zero net flux condition in the equilibrium state at the lower boundary of the plume, i.e.,

$$5 \quad \frac{K}{D} \frac{dc_i}{d\sigma} + w_i c_i = 0, \text{ for } \sigma=1$$

and a Dirichlet boundary condition at the upper boundary, i.e.,

$$c_i = c_{i,b}, \text{ for } \sigma=0$$

where  $c_{i,b}$  is the frazil concentration at the ice shelf/sea ice base, the vertical exponential profile for the equilibrium frazil concentration can be readily obtained (Cheng et al., 2017):

$$10 \quad \frac{c_i(\sigma)}{c_{i,b}} = \exp(-6Z_*),$$

where  $Z_* = w_i/\kappa u_*$  is the suspension index, otherwise known as the Rouse number. Integrating this exponential profile from  $\sigma=0$  to 1, we finally obtain the relation between  $c_i(\sigma)$  and  $C_i$  as

$$\frac{c_i(\sigma)}{C_i} = \frac{6Z_* \exp(-6Z_*\sigma)}{1 - \exp(-6Z_*)}. \quad (2)$$

” (see P4L3-22)

15

*Then again on page 8, line 2, the authors analyze the results in terms of some chosen crystal size class that was dominant in some previous studies. Since the model calculated the size distribution (I think), the authors can interpret their results in terms of it. Picking a particular size class is odd because one of the sensitivity experiments involved changing the size classes (i.e. the discretization of the crystal size distribution). Note that the growth rate depends on crystal size, so a simple average size might not be appropriate.*

20

*In the conclusions, page 10, line 2, the authors mention the ‘complicated form of the relationship depending on suspension index’. I think this relationship might become clearer through thinking about changes to the crystal size distribution.*

*7. Section 4. I felt the explanations could have been clearer. For example, phrases like ‘supercooling is utilised more efficiently’ seem to be key but I didn’t understand precisely what this meant or why it happened.*

25

*9. The figures contained a lot of information so they are necessarily somewhat complicated. However, all figures are particularly difficult to interpret printed in black and white. In figures 7–10, I would have coloured each point according to  $Z_*a$ , rather than dividing into bands. The complicated legends could then be replaced by a simpler colour bar.*

Thank you for these very important comments! We admit that naively picking an intermediate crystal size is unreasonable in this study. However, it is unfortunate that we did not output the size distribution in the steady state before. Consequently, we have rerun the extensive sensitivity experiments to obtain the size distribution information, and have found results that are

30

interesting. We have adopted a new method to calculate  $Z_*$  based on the size distribution information, rather than choosing a particular size class, and have described the method on P9L14-18:

“

We therefore calculated the weighted-average of  $Z_*$  at each grid point for the VM model using the following equation:

$$5 \quad \bar{Z}_* = \frac{\sum_{k=1}^n C_i^k Z_*^k}{\sum_{k=1}^n C_i^k} = \frac{\sum_{k=1}^n C_i^k Z_*^k}{C_i},$$

where  $C_i^k$  is the frazil concentration of the  $k^{\text{th}}$  size class, and  $n$  is the number of size classes used. Then, we took the average of  $\bar{Z}_*$  over all the grid points occupied by the plume to give a representative suspension index for the VM runs (hereinafter  $\bar{Z}_*$  denotes its area-averaged value).

”

- 10 As suggested, we replotted the corresponding figures with each point colour-coded by  $\bar{Z}_*$ , and found more details that are interesting and the reinforce our previous analysis. We have revised the following figures and text:

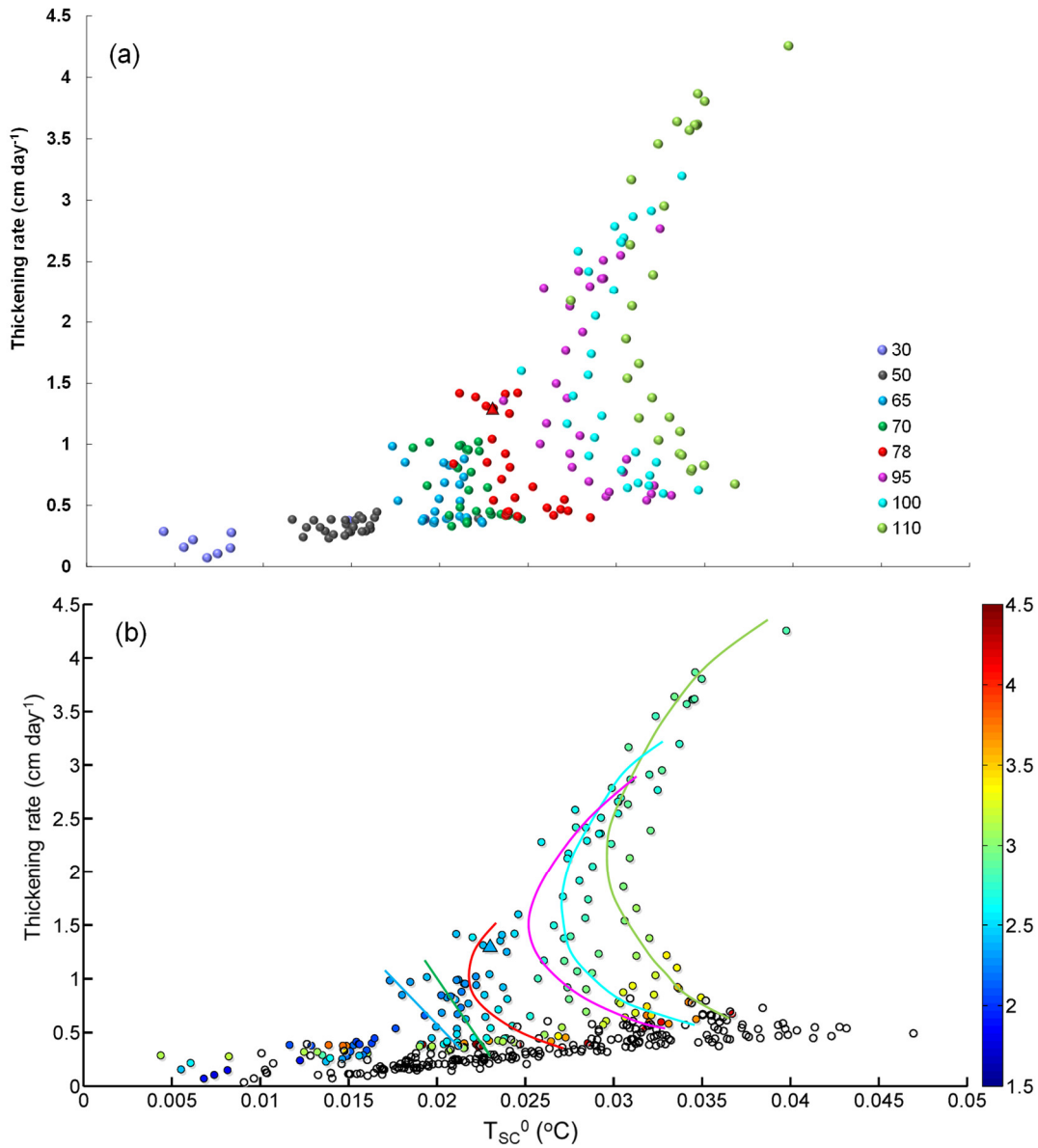


Figure 7: Relationship between  $T_{SC}^0$  and thickening rate classified by (a) outflow supercooled layer thickness  $D_{SC}^{ini}$  and (b)  $\bar{Z}_*$  (colour-coded). Numbers in legend of (a) represent the values of  $D_{SC}^{ini}$ . Solid and hollow dots in (b) correspond to the VM and VU model runs, respectively. Coloured lines depict the central trend of the corresponding data points shown in (a).

5 Triangle corresponds to the standard run. The results are from the last 30 days of the model runs.



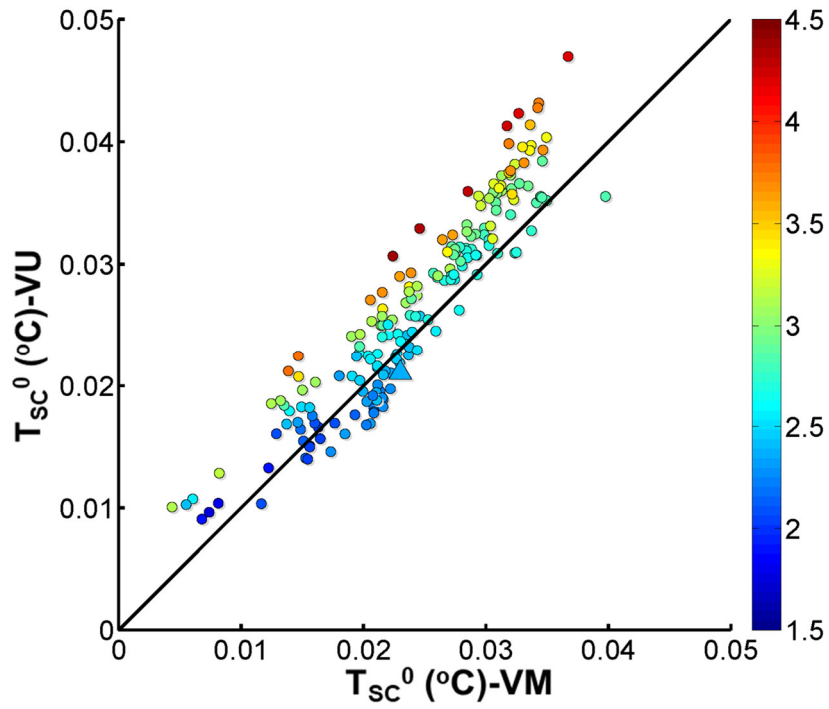


Figure 8: Comparison of  $T_{sc}^0$  calculated by the VM and VU models. Triangle corresponds to the standard run. The colour scale of  $\bar{Z}_*$  is the same as in Figure 7b.

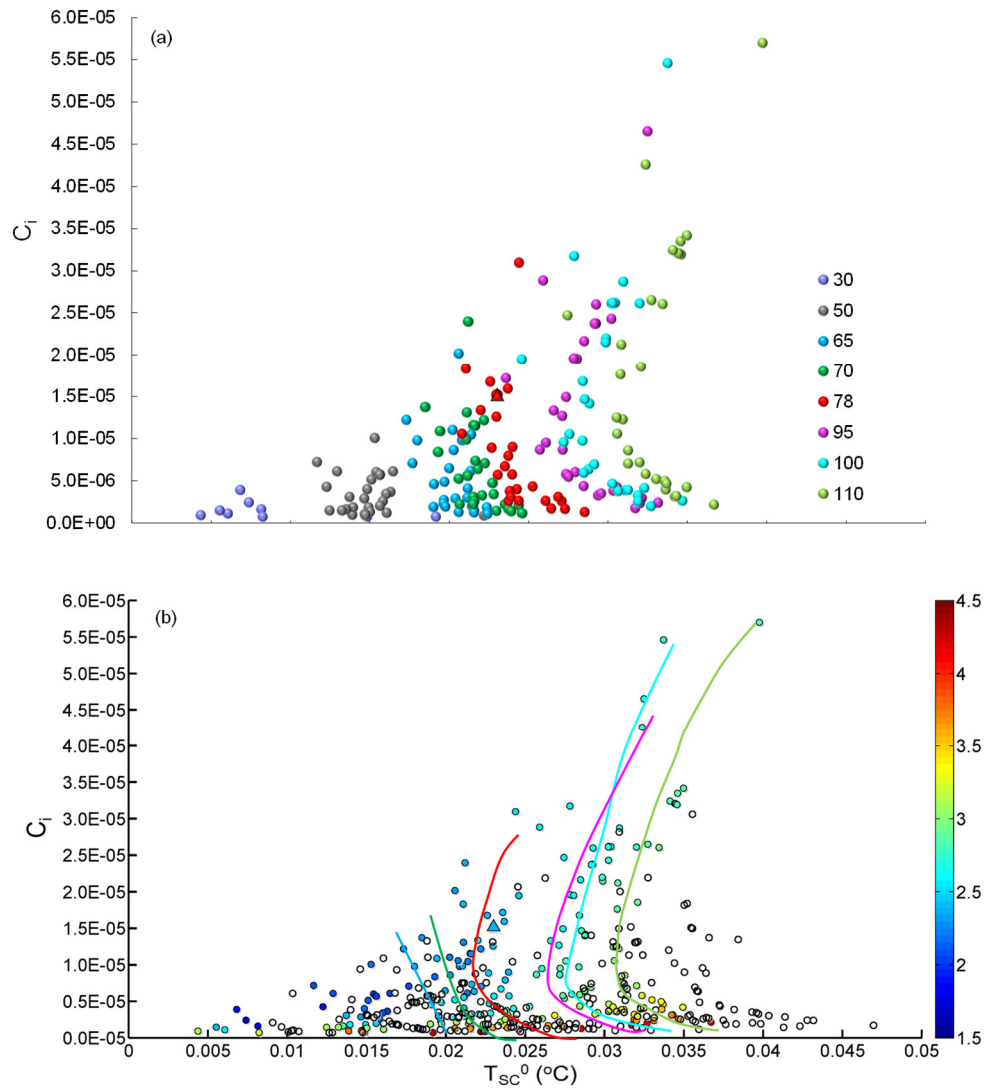


Figure 9: Same as Fig. 7, but for the relationship between  $T_{SC}^0$  and  $C_i$ .

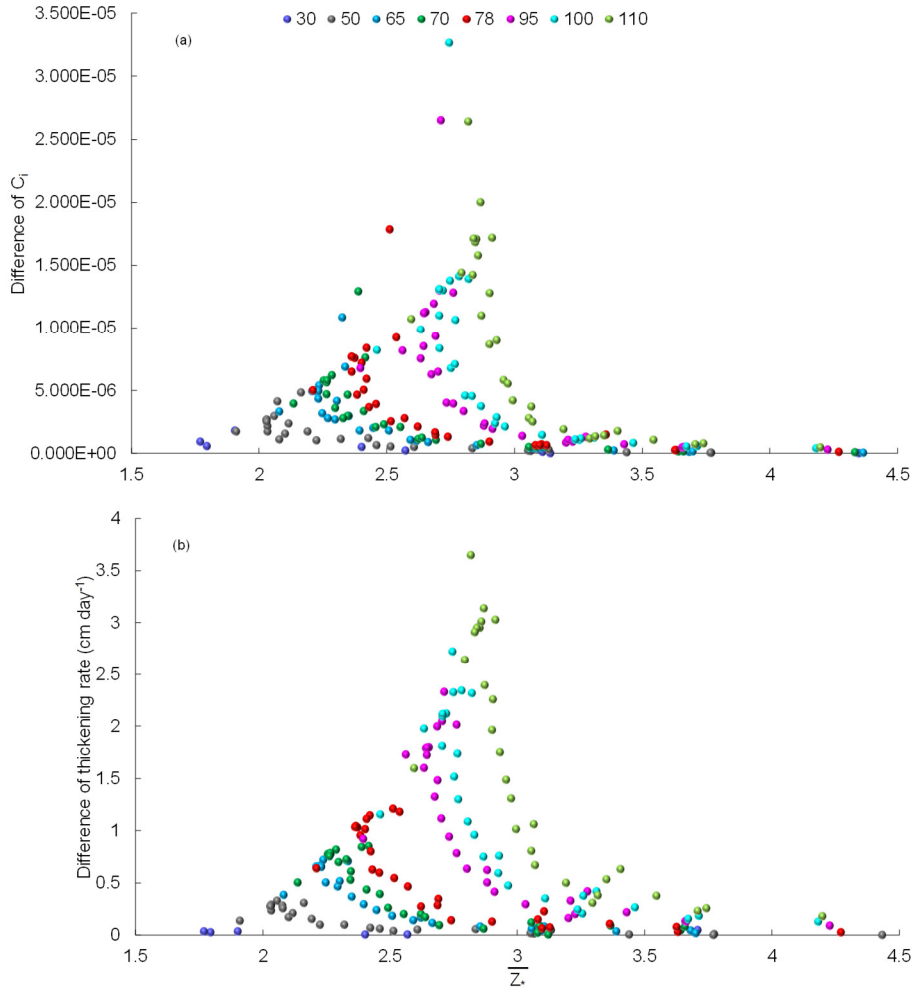


Figure 10: Relationship between  $\bar{Z}_*$  and difference of (a)  $C_i$  and (b) thickening rate calculated by VM and VU models (VM minus VU), classified by outflow supercooled layer thickness  $D_{SC}^{ini}$ . Numbers in legend represent the values of  $D_{SC}^{ini}$ .

“

- 5 We replotted the VM model results characterized by  $\bar{Z}_*$  in Fig. 7b. We find systematic changes in  $\bar{Z}_*$  with increasing thickening rate (along the coloured lines in Fig. 7b), particularly for  $D_{SC}^{ini} \geq 78$  m where the inflexions emerge. With decreasing  $\bar{Z}_*$ ,  $T_{SC}^0$  first decreases, and then increases. If  $\bar{Z}_*$  is sufficiently large, the suspended frazil crystals deposit out of the ISW plume so rapidly that they cannot efficiently use the ISW supercooling to grow, leading to the smallest platelet layer production for the VM model. For smaller  $\bar{Z}_*$ , the frazil crystals bathed in the supercooled layer of the ISW plume can
- 10 remain in suspension and grow longer, resulting in a thicker platelet layer and less residual supercooling. However, if  $\bar{Z}_*$  decreases further, higher frazil concentration occurs within the lower, overheated part of the ISW plume, where melting of the crystals can mitigate the release of latent heat (Fig. 2b). That promotes further growth of frazil ice which can remain in suspension even longer, and thus lead to rapid platelet layer production. The thickening rate calculated by the VU model is

also shown, and is discernibly smaller than that calculated by the VM model. In addition, the maximum values of  $T_{SC}^0$  were obtained within the VU model, because the supercooling is used less efficiently for producing the platelet layer in the VU than in the corresponding VM runs.

5 These arguments can be further illustrated by a more detailed comparison of  $T_{SC}^0$  calculated by the VM and VU models (Fig. 8). There are a number of runs, including the standard run, that have larger  $T_{SC}^0$  values in the VM than in the VU model. The trend from larger  $T_{SC}^0$  in the VM model to larger  $T_{SC}^0$  in the VU model is accompanied by increases in  $\bar{Z}_*$ . When  $\bar{Z}_*$  is relatively small, large frazil concentration exists within the lower overheated part of the ISW plume (Fig. 2b) where melting of frazil ice (causing cooling) counteracts the consumption of supercooling by frazil growth (causing warming) in the upper part of the plume. As  $\bar{Z}_*$  increases, the frazil concentration within the lower overheated part decreases, and finally vanishes, and the resulting release of supercooling in the upper part is more efficient in the VM model, giving larger  $T_{SC}^0$  values in the VU model.

” [P9L18-P10L8](#)

“

15 As expected, the complex response of  $C_i$  to variations in  $T_{SC}^0$  (Fig. 9) is similar to the relationship between  $T_{SC}^0$  and thickening rate (Fig. 7) in the VM model.

” [P10L18-19](#)

As the referee expected, the relationship become clearer through thinking about changes to the crystal size distribution. In addition, we redrew the original Fig. 10 in a more appropriate style:

20 “

The magnitude of the difference in  $C_i$  calculated by VM and VU models (VM minus VU) is compared in Fig. 10a, where we find that  $C_i$  calculated by the VM model is always larger than that calculated by the VU model. In general, the difference increases with decreasing  $\bar{Z}_*$ , while the sensitivity grows with increasing  $D_{SC}^{ini}$ . The dependence on  $\bar{Z}_*$  is once again due to the impact of the combined thermodynamic processes, i.e., the efficient growth in the upper supercooled part of the plume together with the maintenance of supercooling by melting of frazil in the lower part, discussed above. We also see similar behavior for the difference in the thickening rate (Fig. 10b).

25 ” [P10L21-26](#)

5. Page 4, around line 15. There is a pair of papers (Rees Jones and Wells, 2015 & 2018, the latter of which you cite) which  
30 update the treatment of frazil crystal growth/melting.

These interesting studies focus on the details of frazil ice growth in supercooled water, but include no discussion of frazil melting within overheated ambient water. Consequently, the treatment of the melting frazil ice, adopted in this study, remains the best available, and has been widely used in a series of previous studies.

5 Rees Jones and Wells (2015) carried out a simulation of microphysical processes during frazil growth in supercooled water, and their model result is consistent with the parameterization of frazil growth proposed by Jenkins and Bombosch (1995), which considered the aspect ratio of the frazil disc in the growth rate formulation. However, after Jenkins and Bombosch (1995), all subsequent studies did not encapsulate that factor into the frazil ice growth rate. Our formulation is consistent with those later studies.

10 In our study, the relationship between supercooling and thickening rate is strongly controlled by the suspension index that is determined by the drag coefficient (related to  $u_*$ ) and frazil size (related to  $w_i$ ). Our sensitivity experiments using a range of crystal sizes from “A” to “2×A” and different values of drag coefficient effectively characterise that relationship. Changing other parameters, such as  $W_{ini}$ ,  $C_i^{ini}$ ,  $V_a$ ,  $\bar{n}$ , has little impact on the relationship, because the corresponding suspension indices changes little from that in the standard run. Therefore, we would argue that adopting an alternative growth rate formulation would not alter the form of the relationship, despite giving a faster frazil growth rate. That effect is alternatively  
15 captured by using larger frazil ice sizes, as discussed in Rees Jones and Wells (2018), so has been effectively examined in our 211 sensitivity runs.

In summary, we retained the commonly-used formulations for frazil ice growth/melting in order to focus on the impact of the introduction of the vertical profile of frazil ice concentration.

20 *Regarding the need to limit the mass loss due to melting, I think this is a departure from the ‘equilibrium’ (i.e. steady state) assumption in your vertical ice concentration distribution. Because the local melting rate is proportional to local concentration, the ice mass should just approach zero exponentially over time. Or perhaps there is an issue with your time stepping scheme or use of an excessively large time step (how was 25 seconds chosen)?*

25 The concept of an equilibrium vertical profile of frazil ice was introduced from suspended sediment dynamics (Cheng et al., JPO, 2017). However, the equilibrium vertical profile of suspended sediment can hardly be reached in realistic conditions, since the deposition process can make the vertical profile deviate from the equilibrium state (Cheng et al., ESPL, 2016). For suspended frazil ice, not only its melting in the lower overheated part of the ISW plume, but also its growth in the upper supercooled part, make this issue more complicated. Both contribute to the departure from the equilibrium state, in addition  
30 to the deposition process. For this study, introducing the equilibrium vertical profile of frazil ice can be regarded as the leading-order approximation to the non-equilibrium one.

Referring to the time step, it must be very small to reconcile the frazil melting at all grid points in our two-dimensional McMurdo Sound model, because the size distribution and vertical distribution of frazil concentration for each size differ at each grid point. Using a smaller time step can stabilize our models at a price of increased integration time caused by the

multiple-sized frazil ice module. We found that the use of 25 s, with the introduction of the limit on melting, was a good compromise that avoided model instability but also maintained the computational efficiency necessary for our extensive sensitivity experiments.

- 5 6. *Sensitivity experiments. In equation (3), there are a couple of ‘fudge factors’ (solid fraction, volume change) that are not varied. Changing these would be a direct, linear way to get more platelet ice in runs that had less than in observations. Can the authors explain what process the volume change parameter is supposed to represent?*

Both solid fraction and volume change are factors related to the complex processes that take place after the frazil ice precipitates onto the sea ice base. That issue is not our focus, and is not addressed in this study. Therefore, the adopted values for these uncertain factors follow Hughes et al. (2014) that is, to our knowledge, the only literature referring to the simulation of platelet layer thickness in McMurdo Sound based on the ISW plume concept. Setting the solid fraction to 0.25 is observationally supported by Gough et al. (2012), but the volume change factor is quite uncertain. As Hughes et al. (2017) argued, “the subice platelet layer is composed of platelet crystals that, on average, doubled in volume after precipitating. This third factor is a broad estimate, as there appear to be no values from the literature to guide it.”. In view of that, we just kept these two little known factors, not directly related to the frazil-ice-laden ISW plume processes we are concerned with here, constant.

- 20 *More broadly, the authors seem to tune a large range of model parameters. This limits the predictive value of the study since these parameters are unknown a priori. Could these parameters be used elsewhere or would one need to retune each time? Is the greatly increased drag coefficient (for example) plausible?*

The large number of physical and input parameters that need to be tuned, with little observational guidance, is a common feature of models of the sub-ice environment, especially those focussed on frazil ice processes. However, reproducing the observational supercooling level and platelet layer thickness was not the only purpose of our study. More importantly, we aimed to investigate the relationship between supercooling and platelet layer thickening rate, and we expect those results to be more transferable to other geographic locations. We would expect that, if we apply this model elsewhere, such as underneath the ice shelves to simulate the marine ice accretion there, retuning will be necessary, but will be made easier by the knowledge acquired in this study. On the specific point of the drag coefficient, the increased values used here are motivated by the observational evidence from Robinson et al. (2017).

*Some of the sensitivity experiments seem very odd. Particularly changing the frazil size configuration (discretization of the crystal equations in size space). If the distribution were well resolved, changing the discretization wouldn’t change the results. I think the author should use more crystals size classes (at least as a test) and should use a smaller minimum crystal*

size. The minimum size is often very important in these models because it ends up being the size of nucleated crystals. A minimum size of 0.2 mm, therefore, seems large.

Another important comment! “It is unlikely that the natural process of sediment transport by flowing water will be understood in precise dynamical terms in the foreseeable future.”, said R. A. Bagnold (1980), a famous sedimentology scientist. However, as we know, the suspended frazil ice seems to be even more complicated than the suspended sediment because of the thermohaline exchanges, which has a number of uncertainties, including its size configuration. It could be set to an arbitrary configuration, even a single size for some idealized case studies (such as Jordan, J. R., Holland, P. R., Jenkins, A., Piggott, M. D., and Kimura, S.: Modeling ice-ocean interaction in ice-shelf crevasses, *J. Geophys. Res.-Oceans*, 119, 995-1008, <http://doi.org/10.1002/2013JC009208>, 2014 and Jordan, J. R., Kimura, S., Holland, P. R., Jenkins, A., and Piggott, M. D.: On the conditional frazil ice instability in seawater, *J. Phys. Oceanogr.*, 45, 1121-1138, <http://doi.org/10.1175/JPO-D-14-0159.1>, 2015). This is because there is, to our knowledge, no direct observation about the frazil ice size configuration within the boundary layer underneath the ice shelves or the sea ice. However, following the referee’s suggestion, we also conducted an additional 24 model runs with a wider size range, 0.05 to 3 mm divided into 8 classes, i.e., 0.05, 0.2, 0.7, 1.2, 1.7, 2.1, 2.6, and 3 mm, using three values (0.01, 0.02, and 0.03) for the drag coefficient.

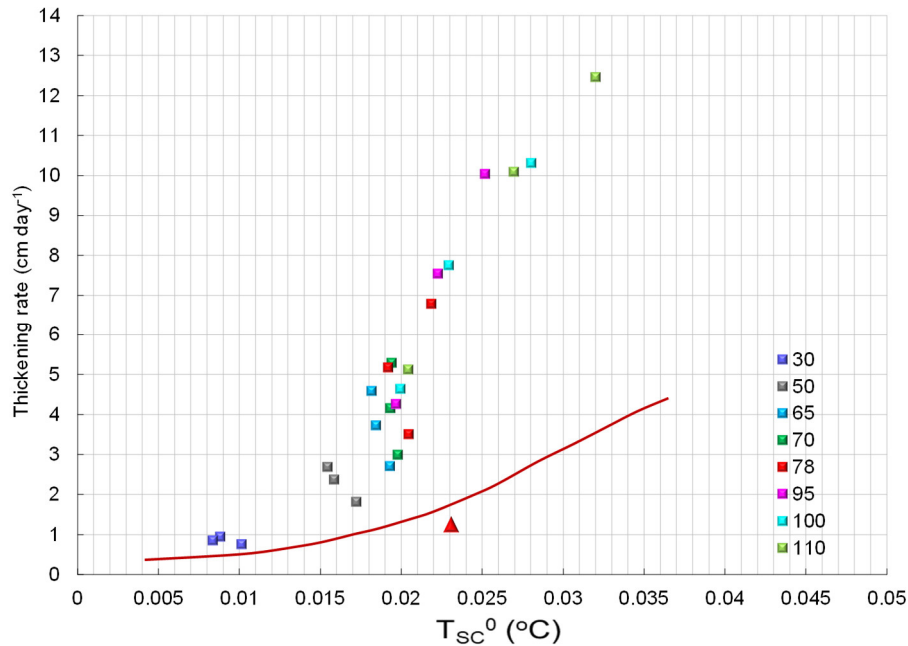


Figure R: Relationship between  $T_{SC}^0$  and thickening rate classified by outflow supercooled layer thickness  $D_{SC}^{ini}$  for the wider size range runs. Red solid line depicts the upper limit of the data points shown in Figure 7 of the paper. Numbers in the legend represent the values of  $D_{SC}^{ini}$ . Triangle corresponds to the standard run.

It can be seen from Fig. R that the thickening rate for the wider size range is well beyond that of all the other runs. The lowest thickening rate for each  $D_{SC}^{ini}$  corresponds to the lower limit of the drag coefficient  $C_D$ , because the low drag coefficient implies weak turbulence so ice crystals can easily be lost by the plume and few reach the lower part of the plume to melt and sustain the supercooling. However, for the wider size range runs, the lower limit of the drag coefficient is set to 0.01 that is also the lower limit of the observational estimates in McMurdo Sound, corresponding to a thin layer of tiny platelets with limited supercooling (Robinson et al., 2017). Although  $D_{SC}^{ini} = 78$  m and  $C_D = 0.01$  give a calculated  $T_{SC}^0$  of 0.02 °C for the wider size range, comparable with that for the standard run (0.023 °C), the thickening rate is 2.7 times larger than that for the standard run, which reproduced the observational supercooling level (Fig. 4a) and platelet layer thickness in McMurdo Sound (Fig. 6a and b). Therefore, in view of that contradiction between the significantly larger platelet layer production than suggested by observations, even using a drag coefficient appropriate for a thin, possibly transient platelet layer (Robinson et al., 2017), we infer that the wider size range gives a poorer representation of conditions in McMurdo Sound and we focus exclusively on the standard size range in our study. Nevertheless, we note that the form of the relationship between  $T_{SC}^0$  and thickening rate shown in Fig. R is consistent with that shown in Fig. 7a when  $D_{SC}^{ini} \geq 65$  m. Furthermore, the decreasing thickening rate transitions to an increasing trend with increasing supercooling for  $D_{SC}^{ini} \geq 78$  m, as for the standard size range runs (Fig. 7a).

Finally, we emphasize that our sensitivity experiments have included runs with changes in the average number of frazil crystals per unit volume, and the minimum crystal size in the standard size range runs is different from each other (Table 3), and both of those will affect the effect process secondary nucleation. However, we find that those parameters have comparatively little impact on our results.

8. *The use of acronyms was excessive for my taste. For example, page 5, line 24 contained five acronyms. I would recommend using more sparingly. Personally, I would change SIPL to 'platelet layer'; FIC to 'frazil concentration'; ASTR to 'thickening rate'. I would change VM and NVM (in any case NVM is an odd name, a double negative, perhaps 'vertically uniform' would be better). In a similar vein, the notation is excessively complicated, with an over-use of 'modifiers' (to give a couple of examples, among many, TSC 0, Z\*a).*

As suggested, we have changed SIPL to 'platelet layer'; FIC to 'frazil concentration'; ASTR to 'thickening rate', and used  $T_{SC}^0$  and  $\bar{Z}_*$  to represent the area-averaged supercooling level at the sea ice base and weighted suspension index, respectively.

### 30 3 Technical comments

1. *Title: I think the paper is broader than just the thickening rate*

Agree. We changed the title to “Responses of sub-ice platelet layer thickening rate and frazil ice concentration to variations in Ice Shelf Water supercooling in McMurdo Sound, Antarctica”



2. *Abstract: I would particularly avoid using so many acronyms in the abstract*

Agree. Following the specific comment above, the abstract contains only one acronym of “ISW”.

3. *Abstract, line 16 ‘choice of frazil ice suspension index’: is it really a choice? The meaning of the term ‘suspension index’ is not clear at this stage.*

5 Agree. We deleted ‘choice of frazil ice suspension index’ and gave a more explicit expression:

“..., and found to be **predominantly controlled by** the vertical distribution of frazil concentration.” (P1L17-18)

4. *Page 1, line 25: maybe delete ‘the’ before ‘elevated pressure’*

Revised

5. *Page 2, line 14: clause that starts ‘in which supercooling’ belongs in or immediately after previous sentence.*

10 Revised

6. *Page 2, line 24: how important are these differences ( $D$  not constant, 2 lateral dimensions) in the context of this paper?*

A variable ISW plume thickness (illustrated in Fig. 5a and b) allows the flow to be controlled by geostrophy. More importantly, we cannot obtain the two-dimensional patterns of hydrographic properties and platelet layer thickness using a one-dimensional model. Therefore, our two-dimensional model is much more appropriate for an investigation of the

15 complex relationship between supercooling and thickening rate in McMurdo Sound.

7. *Page 3, line 5–13: split sentence*

Revised

8. *Page 3, line 6: ‘can be quantified through’ is vague. Perhaps ‘is proportional to’*

Revised

20 9. *Page 3, line 8:  $I_{gr}$  not clearly defined*

We revised the sentence as

“The frazil ice growth rate is found to be proportional to the following integral expression once a number of physical parameters within the commonly-used formulation of Jenkins and Bombosch (1995) are merged:” P3L16-17

10. *Page 3, line 9:  $[0,1]$ , use a comma*

25 Revised

11. *Page 3, line 27: don’t understand  $U_p + U_a$  or  $U_p(U_a)$ ? Similarly with  $V$ .*

The lower surface of the sea ice in McMurdo Sound is regarded as a horizontal plane. Therefore, Hughes et al. (2014) used a combination of the plume velocity and ambient current,  $U_p + U_a$ , to cope with the lack of a sloping ice base along which the buoyant plume ascends. This study follows that treatment.

30 12. *Page 3, line 28: italicize  $x$  and  $y$  (also elsewhere)*

Revised

13. *Page 5, line 7: reads slightly oddly because the ‘outflow’ is actually the inflow to your domain*

We revised “At the outflow the plume thickness ...” as “[The initial thickness of the ISW outflow from underneath McMurdo Ice Shelf ...](#)”.

14. Page 5, line 16: *do you conserve latent heat in this the crystal volume doubling step?*

No. The crystal volume doubling occurs after the frazil ice precipitates out of the ISW plume onto the sea ice base. This process and its potential influences on the underlying ISW plume are not the considered in this study.

15. Page 7, line 4–8: *I suggest that you think about steady state solutions*

Our discussion of the relationship between supercooling and thickening rate focuses on the steady state attained at the end of the model runs.

16. Page 8, line 18: *presumably the consumption of supercooling is by the release of latent heat? If so, I would say this explicitly.*

Revised

17. Page 9, line 13: *‘the differences increase with decreasing  $Z^*a$ ’ seemed odd to me, because  $Z^* = 0$  is supposed to recover the previous models*

As shown in Fig. 2b, VM returns to VU when and only when the suspension index equals zero and the whole ISW plume is vertically supercooled. That means VM never returns to VU in a practical application.

18. Table 1: *some quantities not defined in main text, including  $a_r$ ;  $n$*

“ $a_r$ ” and “ $n$ ” are two parameters associated with the frazil ice melting and secondary nucleation parameterizations and are not repeated in the main text (P5L22-27).

19. Table 1: *Tini seems to be a function of  $z$ , but I thought temperature was vertically averaged in the model?*

20 Sorry for the typographic mistake. We revised the expression of  $T_{ini}$  as  $-0.0573 \times S_{ini} + 0.0832 - 7.61 \times 10^{-4} D_{ini}$ .

20. Figure 3: *annotations like  $p'$  will be impossible to understand unless the reader is very familiar with the frazil literature. I think  $w'$  is more usual than  $\omega'$  for frazil growth.*

The meanings of the annotations  $f'$ ,  $w'$ ,  $N'$ , and  $p'$  are given in the main text, just before Fig. 3 is first referenced (P5L25-26).

We changed  $\omega'$  to  $w'$  in Fig. 3 and the main text.

## Reply to Referee #2:

### *Summary*

5 *This manuscript identifies, and attempts to quantify, the complexity of the interactions between supercooled water, frazil ice held in turbulent suspension, platelet ice accretion and the temporal evolution of Ice Shelf Water plumes originating in the cold cavities of Antarctic ice shelves. The model used is an evolution of earlier models applied to this problem, with the significant point of difference being inhomogeneous vertical profiles of supercooling and frazil-ice concentration.*

10 *In my opinion, the material covered could be of interest to the polar oceanographic community, and its presentation is timely, considering the expansion of interest in the fate of the Antarctic ice shelves and the sea ice affected by their basal melt. However, I do not believe that the stated 'main objective' has been satisfactorily achieved in light of the limitations of the sensitivity studies. I also think that significant clarification is required before the manuscript would be ready for publication.*

We thank the referee #2 for his/her pertinent assessment of our paper and very constructive comments, which have helped us to improve our manuscript. We hope to address all the specific issues below.

15

### *Major Points*

#### *1. Novelty of approach*

*a. The introduction of depth-dependent supercooling and frazil ice concentration was explored in a practical setting by Cheng et al., (2017), so it is not clear that there is a great deal of novelty in the present study.*

20

In Cheng et al. (2017), there is a simple application of VM underneath the western part of Ronne Ice Shelf to demonstrate its improved performance in reproducing the local observed marine ice thickening rate. However, there is no in-depth discussion of the impact of the combined nonlinear effects of the vertical profiles of supercooling and frazil ice concentration. To our knowledge, other than Hughes et al. (2014), there is no numerical modelling study of sub-ice platelet layer growth using the ISW plume concept. We build on that study using a model with two horizontal dimensions, and more importantly, focus on the fundamental relationship between supercooling and platelet layer thickening rate in McMurdo Sound. We show for the first time how that relationship is controlled predominantly by the vertical distribution of frazil concentration.

#### *2. Confusion around terms and purpose*

30 *a. The general purpose of the study appears to be to improve model representation of marine ice accretion beneath ice shelves. That being the case, some justification is required for evaluating the model against an ISW plume beneath sea ice, which is generating a sub-ice platelet layer (as opposed to accreted marine ice). While there is clearly a lot of connection and similarity between these, some explanation of the differences and limitations of applicability need to be provided. For example: the difference in absolute pressure and its consequence for supercooling potential; the effect of basal slope for*

*generating buoyancy-derived momentum; the likely strength of flow and turbulence in the boundary layer and implications for size of crystal held in suspension.*

*b. A comment is also required on the general applicability of a model evaluated against a sub-sea ice ISW plume for the ice shelf cavity.*

5 *c. No definitions of the terms ‘frazil ice’ and ‘platelet ice’ are offered, and direct similarity between sub-ice platelet layers and accreted marine ice is implied. These terms are not interchangeable, and their use here contributes to a general confusion as to the overall purpose of the study. Use of the term ‘platelet-like frazil crystals’ (p1 line 28) exemplifies this confusion (for both the authors and readers). Clear definitions of these terms would help, as would a statement that the plume in McMurdo Sound is being used to evaluate model performance on the basis that it is the most comprehensively*  
10 *observed plume available, despite its expected differences (which should be clearly identified) from a sub-ice shelf ISW plume.*

*e. I find the comment in the Conclusions (p. 10, lines 9 – 11) that “additional observations of supercooled ISW, SIPL and frazil size spectrum in western McMurdo Sound are needed to constrain the relationships determining marine ice formation beneath ice shelves”, rather strange. The recommendation surely should be to observe these parameters beneath ice shelves,*  
15 *if that is indeed the desired outcome?*

We apologize for the confusions between marine ice and platelet layer under the ice shelves and sea ice, respectively, and between frazil ice and platelet ice. Conventionally, we refer to suspended ice crystals within the ISW plume as ‘frazil ice’, and refer to ice accretion underneath ice shelves and sea ice as ‘marine ice’ and ‘platelet layer’, respectively, throughout this  
20 manuscript. In addition, we changed “platelet-like frazil ice crystals” to “[disk-shaped](#) frazil ice crystals”. The general purpose of this study has been given in the previous response, and we only focus on the McMurdo Sound, where there exists a comprehensive observational database for model validation.

We do not entirely agree with the referee’s statements about the distinction between the processes operating beneath ice shelves and platelet ice layers in front of ice shelves. Beneath the platelet ice layers the supercooling is produced by the  
25 pressure drop experience by ISW at it emerges from beneath an ice shelf and rise towards the sea surface, while regions of marine ice accretion beneath ice shelves have typically very low basal slopes. We suggest that the main distinction is likely to be the magnitude of the vertical temperature gradient through the accreted ice. That will primarily affect only the post-depositional processes that we do not consider. The one indirect effect on the ISW plume might be an increased drag coefficient beneath the platelet layer, where more rapid freezing of the deposited crystals may create more irregularity in the  
30 form of the ice-ocean interface.

To clarify these points, we revised the last section as follows:

“

In this study, we demonstrated how the vertical distributions of supercooling and frazil ice concentration within an ISW plume jointly determine the growth of suspended frazil ice, and thus the rate of platelet layer formation [under sea ice and](#)

marine ice beneath ice shelves. A vertically-modified, frazil-ice-laden, ISW plume model which encapsulates these combined nonlinear effects was applied to the McMurdo Sound region, and reproduced the observed ISW supercooling and platelet layer distributions in two horizontal dimensions. Using multiple model runs, the relationship of ISW supercooling to platelet layer thickening rate and frazil concentration in McMurdo Sound was explored, and shown to be dependent on the suspension index that controls the vertical distribution of frazil concentration within the ISW plume. Moreover, when the thickness of a supercooled layer of ISW is large enough, the efficiency of converting ISW supercooling into frazil concentration, and thus platelet layer growth is determined by the suspension index. These findings highlight the need for further observations in McMurdo Sound, particularly focused near the ISW outflow region in the western sound, where the supercooled ISW plume and platelet layer are prominent, and more general observations that help to constrain the frazil size spectrum within the sea ice-ocean boundary layer. In addition, the performance of the VM model in providing reliable estimates of supercooling and frazil ice flux at the platelet layer base makes it an attractive tool for coupling with sea ice models focusing on microscale processes within the bottom layer of the ice (Buffo et al., 2018).

It would be straightforward for the next step to investigate the relationship between supercooling and marine ice thickening rate underneath ice shelves using the VM model. Quantifying this relationship would be the key to parameterizing the process in more complex three-dimensional, primitive equation ocean models, which frequently neglect details of the ice shelf-ocean boundary layer and processes associated with an evolving suspension of frazil ice crystals (Liu et al., 2017; Mueller et al., 2012, 2018). The main difference between the process of marine ice accretion beneath ice shelves and the growth of the sub-ice platelet layer discussed here is likely to be the magnitude of the vertical heat flux that the deposited frazil ice is subjected to. At the base of an ice shelf, typically several hundred meters thick, the vertical temperature gradient is comparatively small, so the deposited crystals form a slushy layer (Engelhardt and Determann, 1987) that slowly consolidates, possibly as much through compaction as freezing. The ice-ocean interface and the associated drag coefficient are therefore likely to be very different to those observed in McMurdo Sound, where the platelet layer appears to comprise a more open matrix of ice and water that consolidates by freezing as heat is lost to the atmosphere. Therefore, the VM model would need to be re-evaluated against observations of sub-ice shelf ISW plumes and the ice shelf-ocean boundary layer. Finally, further process studies, including the influence of the vertical current structure within either the ice shelf or sea ice - ocean boundary layer (Jenkins, 2016; Robinson et al., 2017) could also contribute to improving our understanding of marine ice and platelet layer formation.

” [\\_P11L2-31](#)

Moreover, as suggested we also added a statement that

“..., arguably one of the most comprehensively observed ISW plumes available (HU14; Langhorne et al., 2015; Robinson et al. 2014).” [\\_P2L26-27](#)

d. The general confusion of purpose is demonstrated in that the Abstract opens with the ISW plume in McMurdo Sound (I would argue that the abstract should focus on the model rather than its application), while the Introduction is primarily concerned with the sub-ice shelf regime.

5 As suggested earlier, the VM model used here cannot be claimed to be novel in this study. Therefore, we would argue that the abstract should focus on our findings revealed by applying VM to McMurdo Sound rather than the model itself. Furthermore, a number of papers (Hughes et al., 2014; Langhorne et al., 2015; Robinson et al., 2014, 2017) focused on issues closely related to this study, have discussed ISW plume processes under the ice shelves in their Introductions before the authors focus McMurdo Sound as an analogue. We have done likewise, in order to inform readers unfamiliar with the  
10 related issues about the potential wider applicability of the study.

### 3. Inadequate explanation of sensitivity studies and choice of values for parameters

a. Page 5, Line 26-27 justifies the tuning of parameters to reproduce the observed SIPL and supercooled ISW thicknesses, but we are not given an indication of the strength of this tuning. How do the chosen parameters for the standard run  
15 compare with the observations, and observed range of values?

The large number of physical and input parameters that need to be tuned, with little observational guidance, is a common feature of models of the sub-ice environment, especially those focussed on frazil ice processes. Therefore, the final adopted values for the parameters in the standard run must be determined by trial and error, guided by accumulated experience with  
20 the model. We modified the text to "... , extensive tuning of the least constrained model parameters, including..." P7L9.

b. I would expect that the sensitivity of the model could be just as significant for ar, Nice and solid volume fraction as for the parameters that were included in the sensitivity study. Further testing of the sensitivity to these parameters would be ideal, but at least a statement acknowledging (and justifying) their exclusion is required.

25 The aspect ratio of frazil discs  $a_r$  is usually fixed at 0.02, based loosely on laboratory observations, in frazil-ice-laden ISW plume modeling (Holland and Feltham, 2005, 2006; Hughes et al., 2014; Smedsrud and Jenkins, 2004), and is only associated with frazil ice melting in this study. The relationship between supercooling and thickening rate is strongly controlled by the suspension index that is determined by the drag coefficient (related to  $u_*$ ) and frazil size (related to  $w_i$ ).  
30 Our sensitivity experiments using a range of crystal sizes from "A" to "2×A" and different values of the drag coefficient effectively characterise that relationship. Changing other parameters, such as  $W_{ini}$ ,  $C_i^{ini}$ ,  $V_a$ ,  $\bar{n}$ , has little impact on the relationship, because the corresponding suspension indices change little from that in the standard run. Therefore, since changing the aspect ratio would hardly change the suspension index, we would expect little impact on the key relationships. The number of frazil ice sizes  $N_{ice}$ , is associated with many uncertainties, including the size configuration. Even a single size

has been used for some idealized case studies (such as Jordan, J. R., Holland, P. R., Jenkins, A., Piggott, M. D., and Kimura, S.: Modeling ice-ocean interaction in ice-shelf crevasses, *J. Geophys. Res.-Oceans*, 119, 995-1008, <http://doi.org/10.1002/2013JC009208>, 2014 and Jordan, J. R., Kimura, S., Holland, P. R., Jenkins, A., and Piggott, M. D.: On the conditional frazil ice instability in seawater, *J. Phys. Oceanogr.*, 45, 1121-1138, <http://doi.org/10.1175/JPO-D-14-0159.1>, 2015). This is because there are, to our knowledge, no direct observations of the frazil ice sizes within the boundary layer underneath ice shelves the sea ice. Nevertheless, as a test suggested by Referee #1, we also conducted an additional 24 model runs with a wider size range, 0.05 to 3 mm divided into 8 classes, i.e., 0.05, 0.2, 0.7, 1.2, 1.7, 2.1, 2.6, and 3 mm. The corresponding detail found in [P14L32-P16L19 of this report](#). The solid volume fraction is related to the complex processes that take place after the frazil ice precipitates onto the sea ice base and that are not addressed in this study. It is just a proportionality factor in the calculation of the thickening rate, and does not exert any influence on the frazil-ice-laden ISW plume processes that we are concerned with here.

*c. The role of settling dynamics is clearly significant here (as in sediment studies), but this is not referred to at all.*

*Minor Points*

*The thickness of the accreted platelet layer is a critical parameter for testing the performance of the model. However, the mechanism employed for transferring crystals out of the suspended frazil and into the accreted platelet ice layer is not made explicit.*

We improved the description of the frazil ice precipitation as

“  
We treat the frazil ice precipitation rate  $p'$  as inverted sedimentation and follow the parameterization of McCave and Swift (1976):

$$p' = w_i C_i \left(1 - \frac{U^2}{U_c^2}\right) \times He \left(1 - \frac{U^2}{U_c^2}\right), \quad (3)$$

where  $U_c$  is a critical velocity, above which precipitation cannot occur, determined by Jenkins and Bombosch (1995):

$$U_c^2 = \frac{\theta_i(\rho_0 - \rho_i)g^2 r_e}{\rho_0 C_D},$$

where  $\theta_i$  is the Shields criterion,  $\rho_0$  and  $\rho_i$  are reference seawater and ice densities, respectively,  $g$  is gravity,  $r_e$  is the equivalent radius of a sphere with the same volume as the frazil disk. The frazil ice rise velocity,  $w_i$ , is calculated by Morse and Richard (2009):

$$w_i = \begin{cases} 2.025D_i^{1.621} & \text{if } D_i \leq 1.27 \text{ mm} \\ -0.103D_i^2 + 4.069D_i - 2.024 & \text{if } 1.27 < D_i \leq 7 \text{ mm} \end{cases}$$

where  $D_i = 2r_i$  is the diameter of a frazil crystal in mm. The inclusion of the Heaviside function  $He$  means that negative precipitation (i.e., erosion of previously deposited frazil ice) is not permitted. Because we have no idea about how cohesive the ice crystals are once they have settled, the estimation of an erosion rate would entail additional uncertainties.

The complex processes after the frazil ice precipitates onto the sea ice base are simplified in our model. In order to calculate platelet layer thickness  $D_p$  at the  $n^{\text{th}}$  time interval, we adopt the assumptions of HU14 that solid ice fraction within the platelet layer in McMurdo Sound is 0.25 based on the observational estimation from Gough et al. (2012) and that the ice crystals, on average, double in volume after precipitation:

$$D_p = \frac{1}{0.25} \times 2 \times \sum_{k=1}^n (p'_k \times \Delta t).$$

It should be noted that the volume change factor is a broad estimate, with almost no supporting evidence in the literature to guide it.

” [P6L14-P7L2](#)

10

*The manuscript is rather heavy-handed in its use of acronyms:*

*‘ISW’ is well-known and can be used freely;*

*The reader may need a few reminders of what ‘SIPL’ represents;*

As Referee #1 also suggested, we changed ‘SIPL’ to ‘platelet layer’.

15

*Please expand ‘MMS’ to McMurdo Sound in all cases;*

Revised

*‘FIC’ should not be used, especially as it is variously interchanged with ‘ci’;*

20 As Referee #1 also suggested, we changed ‘FIC’ to ‘frazil concentration’.

*‘VM’ is OK;*

*but ‘NVM’ is non-intuitive;*

As Referee #1 also suggested, we changed ‘NVM’ to ‘VU’ (vertically-uniform).

25

*‘ASTR’ is non-intuitive – is it possible to avoid this altogether?*

As Referee #1 also suggested, we changed ‘ASTR’ to ‘thickening rate’.

*The superscript ‘0’ (as in TOSC) is not explained and left to the reader to figure out.*

30 Revised (“... at the sea ice base ( $T_{SC}^0$ , [superscript “0” denotes the sea ice base](#))...” [P7L22](#)).

*P 1, Line 27: “a necessary condition for ice crystals to form...” either needs a reference or should be removed, as primary nucleation is not thought possible under observed supercooling conditions.*



We deleted the words “form and” from the sentence.

*P 2, Line 5-6: “the SIPL should not be ignored...”. This manuscript is not offering new evidence on the role of the SIPL, so is not the place to be offering this recommendation.*

- 5 We revised “In addition, the presence of the platelet layer can also exert an influence on the estimation of sea ice thickness from freeboard information obtained by satellite altimetry (Price et al., 2014). Thus, the platelet layer should not be ignored when investigating sea ice thickness near an ice shelf front using either numerical models or remote sensing of surface elevation.” to “**Therefore**, the platelet layer should not be ignored when investigating sea ice thickness near an ice shelf front.” (P2L5-6).

10

*P2, Line 8-9: “Owing to the paucity of direct observations...” And yet this manuscript relies heavily on observations collected in McMurdo Sound. I do not feel that the observations available (beyond HU14) are sufficiently acknowledged or applied.*

- 15 We revised “The observations, including both oceanographic and ice core data (Fig. 1), are taken from HU14.” to “**To our knowledge, the data reported by HU14 are the most comprehensive available to evaluate our model, including both oceanographic and ice core data in two horizontal dimensions adjacent to McMurdo Ice Shelf.**” (P7L6-8)

*P2, Line 16-17: There is no marine ice production in McMurdo Sound (this is an example of the general confusion identified above).*

20

We revised the wording to “Consequently, earlier assessments of **either** marine ice **or platelet layer** production in the aforementioned areas may need to be reevaluated.” (P2L23-24)

*P2, Line 25-26: here it is inferred that the ISW plume thickness is allowed to evolve in the present study, but this is not stated explicitly.*

25

We made this explicit by adding an adjective as “The **unsteady** VM and VU models used in this study are ...”. (P5L18)

*P3, Line 5: The statement that “the concentration of suspended frazil ice controls the dynamic and thermodynamic evolution of ISW outflows” requires a reference.*

- 30 Added (P3L15)

*I see that a crystal size distribution, incorporating 5 size classes, is being used. But how this is incorporated is not explicitly stated.*

a. P 5, Line 13: *I am not convinced that the frazil ice crystals should be evenly distributed among size classes. Naively, I would expect a much greater proportion to reside in the smallest size class(es). At the very least, this treatment needs a reference.*

5 The even distribution be cited in Holland and Feltham (2005, 2006), Smedsrud and Jenkins (2004) (added in P6L12). In fact, this treatment is only applied to the ISW outflow boundary, after which the overall size distribution is freely evolving.

b. *Is the smallest size class small enough? (I'm not sure on this). Is there a reference to support this?*

d. *I think more justification is needed on the collapsing of a range of size classes to a single size class for comparative*  
10 *purposes.*

c. *I cannot see anywhere that explicitly states whether crystals move between size classes as they grow/melt; or if and how they are removed from the largest size class to accrete as part of the SIPL.*

Again, the frazil size configuration, including the number of frazil ice sizes  $N_{ice}$  and minimum size, must be set arbitrarily  
15 because of the lack of observations to guide the choices. During the model validation, we have tried many size configurations with a range of settings for the minimum size. However, we found it hard to obtain a good match between the model and observational data using a smaller minimum size. In response to Referee #1's comments we no longer analyse the results in terms of a single size class, but instead characterise the size distribution through the average suspension index. We apologise for not explicitly stating that the frazil crystals grow by transferring between size classes. In fact, in this study, we  
20 adopted a commonly used scheme proposed by Smedsrud and Jenkins (2004) to calculate the transfer processes induced by freezing and melting between different size classes. To make this fact clearer, we added a statement "The frazil ice size distribution is represented by 5 crystal size classes, and the transfer processes, induced by frazil freezing and melting, between different size classes are calculated using the scheme proposed by Smedsrud and Jenkins (2004)." to the model description in P6L9-11.

25

*Which temperature is being used? (i.e. in-situ, potential, conservative: : :) In observations of the ISW plume in question (e.g. Dempsey et al., 2010; Robinson et al, 2014; which the authors make reference to), the upper ocean is homogeneous in potential temperature.*

Potential temperature. The data sets taken from Hughes et al. (2014) in this study also give potential temperature. We have  
30 made that explicit in P5L21.

*I presume that latent heat is being added as ice crystals grow, since the supercooling is variously referred to as being 'released', 'utilized', 'converted' and 'varied'. However, how this is incorporated is not identified or referred to anywhere.*

The governing equations and a variety of parameterizations including the frazil ice growing/melting formulations are not given in the main text, since they are presented in detail in the cited literature, and our implementation follows those descriptions. The following text cites the relevant papers:

“

- 5 Both VM and VU models combine the same commonly-used parameterizations of thermohaline exchanges across the ice–water interfaces, specifically a three-equation formulation (Holland and Jenkins, 1999) for the sea ice base and a two-equation formulation for frazil ice (Galton-Fenzi et al., 2012), with a multiple size–class frazil dynamics model (Smedsrud and Jenkins, 2004), to calculate basal freezing ( $f'$ ) and frazil melting/freezing ( $w'$ ), secondary nucleation ( $N'$ ), and precipitation ( $p'$ ). These processes are summarized in Fig. 3. Rather than repeat all the equations here, we recall some of  
10 them and present how we set up our ISW plume models on the McMurdo Sound domain.

” [P5L22-27](#).

Moreover, this comment is similar with the one proposed by Referee #1:

*16. Page 8, line 18: presumably the consumption of supercooling is by the release of latent heat? If so, I would say this explicitly.*

- 15 We revised the text as “, where melting of the crystals can mitigate [the release of latent heat](#) (Fig. 2b).” [\(P9L25\)](#)

*P3, Line 27: To aid clarification, could the word ‘background’ be changed for ‘ambient’ (current), since this will align with the subscript used in the symbol.*

Revised

20

*P3, Line 28: I take from this that the ‘tidal’ speed is not varying in time, but is effectively just an additional source of kinetic energy?*

Yes. This is the conventional treatment of tidal effects in the literature so far.

- 25 *P 4, Line 8: Please identify where the use of  $D_{SC} = 50$  m is derived from. Is there observational support for this? Or has it come from HU14?*

- Setting  $D_{SC}$  to 50 m is arbitrary, because the aim here is only to give a schematic comparison between the calculated  $I_{gr}$  (i.e., frazil ice growth rate) by the VM and VU formulations shown in Fig. 2b, but is still within the calculated range for the  
30 standard run (Figs. 1, 5c and d). We revised the sentence as “..., where  $D_{SC} = 50$  m ([a value within the calculated range for the standard run, Fig. 1](#)) in all the cases.” [\(P5L2\)](#)

*P 4, Line 13-14: I am confused as to why you would want to avoid frazil melting in the lower part of the plume if it is overheated.*

Sorry for this puzzling expression. We revised the text “for given supercooling, in order to avoid frazil melting in the lower, overheated part of the ISW plume,  $Z_*$  must be large enough to maintain greater frazil concentration in the upper, supercooled part.” as “..., if  $Z_*$  becomes larger, there is higher (lower) frazil concentration in the upper (lower), supercooled (overheated) part of the ISW plume.” (P5L8-9)

5

*P 5, Eqn (3): the fact that individual ice crystals may double in volume after precipitation shouldn't affect the thickness of the SIPL, since presumably their growth is into the interstitial spaces, and shouldn't cause the entire SIPL to expand?*

The volume change factor related to the complex processes after the frazil ice precipitates onto the sea ice base is not the issue we focus on, and cannot be addressed in this study. Therefore, the adopted value for this uncertain factor simply follows Hughes et al. (2014) that is, to our knowledge, the only study of platelet layer thickness in McMurdo Sound based on the ISW plume concept. How the growth of deposited individual ice crystals affects the sub-ice platelet layer is not clear. As Hughes et al. (2014) argued, “the subice platelet layer is composed of platelet crystals that, on average, doubled in volume after precipitating. This third factor is a broad estimate, as there appear to be no values from the literature to guide it.”

15

*P5, Line 8: My understanding is that the ‘background circulation’ applied in HU14 was to provide the buoyancy-driven momentum that the sub-IS plume would naturally possess, but which cannot arise automatically within a model beneath a horizontal ice base (i.e. sea ice). That being the case, this represents a departure from sub-Ice Shelf applications, and should be explained again here.*

20

Buoyancy-driven flow beneath a horizontal ice base can be simulated if terms involving the gradient in plume thickness and/or density are introduced into the momentum balance. HU14 did not do that, so the “background circulation” was introduced to provide a flow. We added further clarification of that point to the text: “...: the former, which represented the only source of momentum in the study of HU14, is...” (P6L5)

25

*P 6, Line 10-11: I am not satisfied that there is sufficient support for the statement that ‘both models reproduce the observed values of ISW supercooling reasonably well’. Looking at Figure 4a,*

*a. The structural difference between sites FN and NN is not captured at all;*

*b. The neap-tide supercooling at site C is very different to the modelled result, and the difference between spring and neap at that site is not reflected in the model timeseries;*

30

*c. The observed values at Site W do not coincide with the model timeseries values;*

*d. The only site that has ‘reasonable’ agreement is Site I, which is very close to the inflow point of the prescribed ISW plume.*

We admit all of the model discrepancies mentioned above, and would argue that they arise from the limitations in our model setup that we now explicitly refer to in the text:

“

It can be seen that at the end of the simulations both VM and VU models reproduce the observed reduction in ISW supercooling at the sea ice base ( $T_{SC}^0$ , superscript “0” denotes the sea ice base) in the cross- and long-sound directions, in spite of some evident model discrepancies (Fig. 4a) that may result from the limitations in our model setup: both the ambient current and tides are treated as temporally and spatially constant; there are no long-term observations of ISW outflow to provide reliable boundary conditions; we use a constant drag coefficient, ignoring the spatiotemporal evolution of the sea ice basal form characterized by the platelet layer. Nevertheless, the SS of  $T_{SC}^0$  calculated using VM and VU models are 0.56 and 0.58, respectively, and the CC and RMSE are also reasonable (Table 2).

” P7L21-27

*Also, the spatial resolution in the figures, especially of the ISW plume structure and SIPL thickness (figures 5 and 6) seem to greatly exceed the stated resolution of the model (1 km, P 5, Line 12). This then has implications for the statements made about how these are resolved by the model (as in P 6, Line 29). Also, this seems like fairly low resolution for the ISW plume itself, at 3 km wide.*

The colour map shown in Figs. 5 and 6 is interpolated from our model results using a Natural Neighbour method. We added this statement to the captions of Figs. 5 and 6. In addition, we still believe that “Such small-scale features in the platelet layer thickness distribution, if present, were not resolved by the relatively coarse spatial distribution of ice-core sampling (dots in Fig. 6). Nevertheless, the platelet layer thickness calculated by the VM model at drill sites agrees well with the measurements (Fig. 6a), ...” (P8L13-15), because the resolution of our models, i.e.,  $1 \times 1$  km, is significantly higher than that of the ice-core sampling. The figure of ‘3 km wide’ refers to the initial width of the ISW plume at the outflow. Downstream, the ISW plume extends all along the ‘a-b’ boundary in the steady state (Fig. 5). Therefore, to avoid this misunderstanding, we revised the descriptions of  $D_{ini}(D_{SC}^{ini})$  and  $W_{ini}$  in Table 1 as “Constant ISW plume outflow thickness (constant outflow supercooled layer thickness)” and “ISW plume outflow width with constant  $D_{ini}(D_{SC}^{ini})$ ”, respectively.

*P 7, Line 27ff: Behavior around the ‘inflexion’ points is particularly interesting. I think it would greatly strengthen the paper if the inflexion points could be investigated in higher resolution (especially in  $Z^*$  and  $\sigma_{SC}$ ) to the point where the mechanism causing them could be adequately explained. There is an informal explanation offered in lines 28 – 30, but studying this in greater detail could be very useful for determining if this is a model artefact or a real phenomenon that could invite observational investigation.*

*P 9 Line 8: The sentence is incomplete? Perhaps “: : : there are analogous inflexion points: : :”?*

Thank you for these suggestions. Following Referee #1's related comments, we modified the paper significantly to reinforce our analysis on the inflexions. We adopted a new method to calculate  $Z_*$  which involves the size distribution information, rather than choosing a particular size class, enabling us to analyze our results in terms of this new representative suspension index. We then redrew the corresponding figures with each point colour-coded by the new representative suspension index rather than dividing into bands, and found more details that are interesting and beneficial for our discussion. See our earlier response to Referee #1's related comment (P?L? of this response):

5  
20 *P 8, lines 9-10: perhaps the wording could be more straightforward? Suggest using "... because the supercooling is used less efficiently for producing SIPL in the NVM than in the corresponding VM runs."*

Revised

*P 8/9 How do the critical thicknesses of the supercooled portion of the ISW plume (65 and 78 m) compare with observed thicknesses of the McMurdo Sound ISW plume?*

15

There are no direct observations of the ISW outflow from underneath McMurdo Ice Shelf. Nevertheless, as we have mentioned in the main text (P9L7-8), "...  $D_{SC}^{ini} = 65$  m is the value estimated by HU14 based on the measurements conducted by Lewis and Perkin (1985) and Jones and Hill (2001)."

20 *P 9 Line 24: The sentence is incomplete? ": : : that have been taken instruments not specifically designed: : :"*

Revised

*P10 Line 14-15: Robinson et al. (2017) is an example of such a process study and could be referenced here.*

Added

25

*Table 1: Is there support in the literature for choosing  $ar = 0.02$ ?*

Yes. We have mentioned in the response to comment 3-b: "The aspect ratio of frazil discs  $a_r$  is usually fixed at 0.02, based loosely on laboratory observations, in frazil-ice-laden ISW plume modeling (Holland and Feltham, 2005, 2006; Hughes et al., 2014; Smedsrud and Jenkins, 2004), ..."

30

*Table 3: Could the names of the variables be repeated here so that the table is self contained?*

Revised

*Figure 1: Why does the model data only extend as far as the borehole domain, and not to the edges of the model domain?*

Revised as suggested.

*Figure 1: Do the location names (C, I, W, NN, FN) mean anything in the present study? If yes, can these be provided? If no, could they be simplified to A -> E without loss of generality?*

5 The location names follow Hughes et al. (2014), and we added their definition to the caption of Fig. 1

*Figure 1 caption: The 'oceanographic and SIPL data' are not shown in the figure, so reference to them should be removed from the caption. Unless what is meant are the locations of the oceanographic and SIPL data?*

Removed

10

*Figure 2b: The almost-vertical blue line to the right, and horizontal blue line along the x-axis appear to be mistakes?*

Sorry, we do not find these mistakes in Fig. 2b. Maybe a different edition of PDF software?

*Figure 2b: It would be helpful to add the words 'Melt' and 'Freeze' alongside the appropriate parts of the y-axis. Also, I think that the change of vertical scale is not necessary (and possibly only adds confusion)*

15

We added the necessary words. It should be noted that the negative (melting) integral value is an order of magnitude larger than the positive (freezing) one, so if the vertical scale is unified, the positive part becomes very compressed.

*Figure 3 caption: “: : : relevant processes within a supercooled ISW plume of homogeneous temperature and salinity”.*

20 Revised

*Figure 6: Just a suggestion: it would aid comparison if the location dots could be colored by the measured SIPL thickness.*

Revised

25 *Figure 7a: There is no explicit specification of what 'VM30' through 'VM110' refers to.*

Added to the caption of Fig. 7

*Figure 7a and 7b: Text says that the ASTR estimate is from the last 30 days of the model runs. This needs to be repeated here.*

Added

30

*Also, converting the ASTR to cm/day may be a more useful unit (and less misleading, given that it only refers to 30 days' worth of growth)*

Revised

*Figure 9: The formulae for the fitted lines could be moved out to the right so as not to become lost amongst the data points.*

Fig. 9 has been modified (see earlier response to Referee #1).

*Figure 10: I don't think the additional enlargements provide any further useful information and could be removed.*

5 *Figure 10: Numbers on axes are too small.*

Fig. 10 and the accompanying text have been modified (see earlier response to Referee #1).



## Reply to Ken Hughes

I (Ken Hughes) was lead author of the paper on which a number of comparisons are made in the current manuscript. Consequently, I have a unique perspective on this paper. I have included a number of comments that would improve the clarity of the manuscript, which I read with interest. I am not, however, an official reviewer, and so am providing these comments for the authors' reference.

The authors modify an existing two-dimensional, time integrated ISW plume model to (i) test its ability to recreate observed supercooling and SIPL thickness observations and (ii) via a rigorous sensitivity study, investigate which parameters have disproportionate influence on the spatial distributions.

The idea behind the study is worthwhile as McMurdo Sound provides arguably the best location against which an ISW plume model can be test. Indeed, the two-dimensional model is a noticeable improvement over the 1D approach used by Hughes et al. (2014).

First, we thank Ken for his paper (Hughes et al., 2014) greatly helping us complete this study. We also thank Ken for his pertinent assessment of our paper and very constructive comments, which have helped us to improve our manuscript. We hope to address all the specific issues below.

### Major issues

Line 5.27 "some tuning of model parameters" overlooks some key details

1. Why is the outflow only 3km? Observations in Hughes et al have ISW outflow adjacent to the ice shelf across the whole Sound.

We experimented with a range of different outflow widths, and found that 3 km gave the best match to observations of platelet layer thickness. The plume rapidly spread across the width of the domain (Figure 5), so the results are consistent with the observations of HU14.

2. There is no mention that frazil ice classes in this paper are well below the mode size predicted by Hughes et al. (2014) of 2.5mm radius

It is hard to compare directly the frazil ice classes of this study with those of HU14 in view of the many differences both in the treatment of the plume dynamics and the frazil ice processes. Since the crystal size required to reproduce platelet layer thickness is so strongly dependent on these other aspects of the model, and there are no observations of the dimensions of suspended crystals, we chose not to emphasize these differences in model setup.

Line 2.25 Somewhere in the paper, a description of the plume dynamics beneath the sea ice is warranted. Hughes et al. (2014) used a constant plume thickness out of necessity, because one-dimensional models can't easily deal with a lack of forcing (ie a gravitational component beneath a slope). It appears from Figure 1 that the plume in this paper tends toward geostrophic balance. Is this true? Put another way, does having two spatial dimensions and the time dimension avoid the issues faced by Hughes et al.

Adding terms to the momentum balance that include the horizontal gradients of plume thickness and/or density avoids the issue. That cannot be done in one-dimensional models, although it adds complexity. Adding the second horizontal dimension allows the spatial distribution of the platelet layer to be simulated. We added a statement that “Finally, it can be seen that in both models the ISW plume flow is predominantly governed by a geostrophic balance (Fig 5a-d).” (see P8L1-2)

Line 6.29 Although the overall spatial distribution of SIPL may be graded as "excellent", it predicts a large areas where the thickness is 15m, twice the observations. Similarly, the "poorly" graded NVM model is closer to observations near the outflow. In other words, comparison between the models in terms of SIPL is not a simple as calling one "excellent" and the other "poor".

As we have stated in the main text, the coarse resolution of the ice-core sampling cannot resolve the simulated high gradient of platelet layer thickness near the ISW outflow. It remains unknown whether such sharp gradients exist. Where observations exist, the VM model has superior performance in reproducing the platelet layer thickness, compared with the performance of VU model.

There is no citation, let alone discussion, of Holland and Feltham (2005, doi:10.1017/S002211200400285X), which specifically deals with the issue of the vertical distribution of frazil ice.

This point is consistent with one of the Referee #1's comments. We have now cited this paper in P2L21-23: “Idealized one dimensional models confirm that the vertical distribution of frazil concentration cannot remain well-mixed in the upper layers of the ocean (Svensson and Omstedt, 1998) and beneath ice shelves (Holland and Feltham, 2005).”

On a similar note, there appears to be no real attempt to constrain  $Z^*$ , the suspension index. A large range is proposed, but the reader is not given any idea what a reasonable value is.

The major purpose of this study is to investigate the relationship between the supercooling and platelet layer thickening rate in McMurdo Sound. This complicated relationship is strongly controlled by the frazil ice suspension index. To this end, we

highlight the need to improve frazil ice observations within the sea ice-ocean boundary layer in McMurdo Sound, in order to provide some constraint on the suspension index.

*Minor issues*

5 *Line 1.13: this is not a new frazil-ice-laden ISW plume model, but rather an existing ISW plume model with an improved frazil-ice treatment.*

We changed “new” to “vertically-modified”.

10 *Line 1.15: This sentence should be written as the dependence of supercooling in MMS on the SIPL thickening rate, not the other way as it is currently. In other words, the current sentence says the dependence of x on y is investigated, yet two sentences later, it says x can be expressed as a function of y.*

*Alternatively, reword to something like "Using this model, we test how ISW supercooling in MMS influences SIPL thickening rate".*

*This issue also arises for the heading of Section 4.2*

15

We intended to discuss the dependence of platelet layer thickening rate and depth-averaged frazil ice concentration on ISW supercooling in McMurdo Sound. The sentence “For each suspension index, SIPL thickening rate can be expressed as an exponential function of ISW supercooling.”, has been removed, as a result of other changes in the main text (see our response to the comments of Referees #1 and #2 in detail).

20

*Line 2.10 A reference to Galton-Fenzi et al. (2012) is warranted in this paragraph as they develop a three-dimensional model with frazil ice dynamics. It is not a plume model, per se, but it does involve a non-vertically-uniform approach to frazil ice dynamics.*

Added in **P2L10-11**.

25

*Line 2.16 There is a slight issue with using MMS as an example for areas where marine ice production should be reassessed as it is no longer termed marine ice beneath sea ice.*

30 This comment is similar to one of the major concerns of Referee #2. We are sorry for the blended usage of these specific terms in this study. The revised paper now, consistently refers to suspended ice crystals within the ISW plume as ‘frazil ice’, and to ice accretion underneath ice shelves and sea ice as ‘marine ice’ and ‘platelet layer’, respectively.

*Line 3.16 Hughes et al. (2014) improved upon the method of using  $T_{sc}$  at mid-depth. This is noted by Cheng et al. (2017) but is not noted here.*

We added the following statement “It is worth mentioning that in order to take the supercooling into account when  $\sigma_{SC} < 0.5$ , HU14 integrated  $T_{SC}$  over the supercooled part only without introducing any frazil ice melting. However, in this study, we will demonstrate that the important role of frazil ice melting in the lower, overheated part of the plume cannot be ignored.”

5 (see P3L29-31)

*Line 4.30 Standard notation for ISW plume models has basal freezing as  $m'$  and frazil ice growth as  $f'$ . Is there a reason that here basal freezing is  $f'$  and frazil ice growth is  $\omega'$ ?*

10 Because the basal freezing occurs throughout McMurdo Sound, we think “ $f'$ ” is more appropriate than “ $m'$ ” in this study, consistent with “freezing”. As Referee #1 suggested, we used “ $w'$ ” instead of “ $\omega'$ ” to represent frazil ice growth/melting.

*Line 7.11 Describe the type of observations and model results. Something like “... investigated with satellite altimetry and two-dimensional model results.” (with the actual adjectives based on the respective, cited papers)*

15 Revised as suggested. However, not all cited papers correspond to two-dimensional models, so we used “numerical models”.

# Responses of sub-ice platelet layer thickening rate and frazil ice concentration to variations in Ice Shelf Water supercooling in McMurdo Sound, Antarctica

Chen Cheng<sup>1,2,3</sup>, Adrian Jenkins<sup>2</sup>, Paul R. Holland<sup>2</sup>, Zhaomin Wang<sup>4</sup>, Chengyan Liu<sup>4,1,3</sup>, and Ruibin Xia<sup>1,3</sup>

<sup>1</sup>Polar Climate System and Global Change Laboratory, Nanjing University of Information Science & Technology, Nanjing, 210044, China

<sup>2</sup>British Antarctic Survey, Cambridge, CB3 0ET, UK

<sup>3</sup>School of Marine Sciences, Nanjing University of Information Science & Technology, Nanjing, 210044, China

<sup>4</sup>College of Oceanography, Hohai University, Nanjing, 210098, China

*Correspondence to: Zhaomin Wang (zhaomin.wang@hhu.edu.cn)*

**Abstract.** Persistent outflow of supercooled Ice Shelf Water (ISW) from beneath McMurdo Ice Shelf creates a rapidly growing sub-ice platelet layer having a unique crystallographic structure under the sea ice in McMurdo Sound, Antarctica. A vertically-modified frazil-ice-laden ISW plume model that encapsulates the combined nonlinear effects of the vertical distributions of supercooling and frazil concentration on frazil ice growth is applied to McMurdo Sound, and is shown to reproduce the observed ISW supercooling and platelet layer distributions. Using this model, the dependence of platelet layer thickening rate and depth-averaged frazil ice concentration on ISW supercooling in McMurdo Sound is investigated, and found to be predominantly controlled by the vertical distribution of frazil concentration. The complex dependence on frazil concentration highlights the need to improve frazil ice observations within the sea ice-ocean boundary layer in McMurdo Sound.

## 1 Introduction

Ice shelf basal melting removes more mass from the Antarctic Ice Sheet than iceberg calving does, but the three largest ice shelves, Filchner-Ronne, Ross, and Amery, contribute only 18% of the net meltwater flux (Rignot et al., 2013). That is because the seawater-filled cavities beneath those ice shelves are dominated by High Salinity Shelf Water that has a potential temperature at or near the surface freezing point. Ice shelf basal melting occurs at depth, because the freezing point temperature is lower under elevated pressure, and results in the formation of Ice Shelf Water (ISW), characterized by temperatures below the surface freezing point. When the buoyant ISW ascends along the ice shelf base, the pressure relief causes it to become supercooled in situ, a necessary condition for ice crystals to persist in suspension. Those disk-shaped frazil ice crystals accumulate under the ice shelves, leading to the formation of marine ice that is thicker and more localized than would be possible through direct freezing at the ice shelf base (Morgan, 1972; Oerter et al. 1992; Fricker et al., 2001;

Holland et al., 2007, 2009). Occasionally, frazil ice crystals bathed in supercooled ISW are also carried out beyond the ice shelf front and precipitated under adjacent sea ice, forming an unconsolidated, porous, sub-ice platelet layer (Hunkeler et al., 2016; Langhorne et al., 2015; Leonard et al., 2006; Robinson et al., 2014). The platelet layer not only harbours some of the highest concentrations of sea ice algae on Earth (Arrigo et al., 2010) but also contributes to the sea ice thickness when the water within the pores of the platelet layer freezes to become incorporated ice (Smith et al., 2001). **Therefore**, the platelet layer should not be ignored when investigating sea ice thickness near an ice shelf front.

Owing to the paucity of direct observation, our understanding of the evolution of frazil-ice-laden ISW relies heavily on numerical models. Those models are mostly derived from plume theory (Holland and Feltham, 2006; Jenkins and Bombosch, 1995; Rees Jones and Wells, 2018; Smedsrud and Jenkins, 2004), **but include three-dimensional ocean circulation models (Galton-Fenzi et al., 2012)**, and have been widely applied to assess the marine ice beneath Filchner-Ronne (Bombosch and Jenkins, 1995; Holland et al., 2007; Smedsrud and Jenkins, 2004), Larsen (Holland et al., 2009) **and Amery ice shelves (Galton-Fenzi et al., 2012)**, and the **platelet layer** under the sea ice in McMurdo Sound (Hughes et al., 2014, hereinafter HU14). To date, all the ISW plume models **mentioned above** have been depth-integrated, and all the **scalar quantities, i.e., water temperature, salinity, and frazil concentration** in those models are treated as vertically-uniform. **The well-mixed temperature and salinity have been validated by borehole observations beneath the Amery Ice Shelf (Herraiz-Borreguero et al., 2013) and under the sea ice in McMurdo Sound (Robinson et al., 2014; HU14). Although there are no observations of the vertical profile of frazil ice concentration, it is unlikely to be vertically uniform because the buoyant rise of the crystals will counteract the turbulent diffusion that tends to homogenise the other properties.** Recently, Cheng et al. (2017) showed that **adopting an approach in which the frazil ice growth is calculated using a vertically-uniform frazil concentration** results in substantial underestimation of marine ice production **underneath the western side of Ronne Ice Shelf. Idealized one dimensional models confirm that the vertical distribution of frazil concentration cannot remain well-mixed in the upper layers of the ocean (Svensson and Omstedt, 1998) and beneath ice shelves (Holland and Feltham, 2005).** Consequently, earlier assessments of **either marine ice or platelet layer** production in the aforementioned areas may need to be reevaluated.

McMurdo Sound, located in the southwestern Ross Sea (Fig. 1), is characterized by significant ISW outflow, **arguably one of the most comprehensively observed ISW plumes available (HU14; Langhorne et al., 2015; Robinson et al. 2014).** A prominent platelet layer forms in the central-western sound (Dempsey et al., 2010); the maximum (area-averaged) observational first-year sea ice and platelet layer thickness are 2.5 (2) and 8 (3) m as determined from ice cores recovered adjacent to McMurdo Ice Shelf front between late November and early December in 2011 (Fig. 9 in HU14). The thin (~20 m) McMurdo Ice Shelf front allows the ISW outflow to be delivered to the ocean surface without mixing with warmer ambient waters (Robinson et al., 2014). The study documented in HU14 was the first to apply the steady, one-dimensional frazil-ice-laden ISW plume model developed by Smedsrud and Jenkins (2004) to McMurdo Sound, although a constant ISW plume thickness was used. McMurdo Sound therefore seems an ideal setting in which to apply and evaluate the new vertically-

modified ISW plume model proposed by Cheng et al. (2017), which includes time dependence and two horizontal dimensions. The main objective is to quantify for the first time the response of the platelet layer thickening rate to variations in ISW supercooling. Establishing such a relationship is of significance to the assessment of total sea ice thickness, and thus the oceanic heat flux associated with the platelet layer, in McMurdo Sound and elsewhere.

5

Here we first analyze the combined nonlinear effects of the vertical distributions of supercooling and frazil concentration on the suspended frazil ice growth rate in a supercooled ISW plume, and compare results with those obtained with a commonly-used, depth-averaged formulation. Then, we evaluate the performance of the vertically-modified ISW plume model in reproducing the observed ISW supercooling and platelet layer distribution to show the importance of considering the combined nonlinear effects. Finally, we conduct 211 sensitivity simulations with the purpose of quantitatively establishing the response of the platelet layer thickening rate **as well as the frazil ice concentration** to variations in ISW supercooling in McMurdo Sound.

10

## 2 Physically-based formulation for frazil ice growth rate

The growth rate of suspended frazil ice controls both the dynamic and thermodynamic evolution of ISW plumes and the accretion of ice crystals beneath ice shelves (Cheng et al., 2017; Holland and Feltham, 2006; Smedsrud and Jenkins, 2004) and sea ice (HU14). The frazil ice growth rate is found to be proportional to the following integral expression once a number of physical parameters within the commonly-used formulation of Jenkins and Bombosch (1995) are merged:

15

$$I_{gr} = \int_0^1 T_{SC} c_i(\sigma) d\sigma, \quad T_{SC} = T_f(\sigma, S) - T, \quad (1)$$

where  $\sigma \in [0, 1]$  is the relative vertical coordinate, with 0 and 1 respectively corresponding to the upper ice-plume and lower plume-ambient water interfaces,  $T$  and  $S$  are respectively the plume's temperature and salinity, vertically well-mixed within the plume,  $c_i$  is the vertically-distributed, in this study, volumetric frazil concentration within the plume,  $T_{SC}$  and  $T_f$  are respectively the supercooling level (positive for supercooling) and local freezing point. Because of the well-known linear decrease in  $T_f$  with increasing water depth,  $T_{SC}$  also varies linearly with depth, transitioning from supercooling to overheating as  $\sigma$  increases (Figs. 2a and 3). The corresponding transition height at which  $T_{SC} = 0$  is defined by supercooled thickness  $D_{SC} = \sigma_{SC} D$  where  $\sigma_{SC}$  and  $D$  are respectively supercooled fraction and total ISW plume thickness.

20

25

In earlier ISW plume models, because  $c_i$  is treated as vertically-uniform, the integral of (1) can be represented by the product of the depth-averaged values  $T_{SC}^{0.5}$  (0.5 means at mid-depth) and  $C_i$ . Thus, we refer to these ISW plume models as vertically-uniform (VU). It is worth mentioning that in order to take the supercooling into account when  $\sigma_{SC} < 0.5$ , HU14 integrated  $T_{SC}$  over the supercooled part only without introducing any frazil ice melting. However, in this study, we will demonstrate that the important role of frazil ice melting in the lower, overheated part of the plume cannot be ignored.

30

The vertical distribution of frazil concentration, in reality, much like the concentration of suspended sediment (Cheng et al., 2013, 2016), should be vertically non-uniform, with higher concentrations near the ice shelf/sea ice base. Considering only the balance between the buoyant-rise-induced vertical advection and turbulent diffusion terms, the governing equation for frazil concentration can be written as

$$\frac{d}{d\sigma} \frac{K}{D} \frac{dc_i}{d\sigma} + w_i \frac{dc_i}{d\sigma} = 0,$$

where  $w_i$  is the frazil ice rise velocity, determined by ice crystal size,  $K$  is the vertical frazil concentration diffusion coefficient, which can be parameterized as vertically constant (Cheng et al., 2013, 2016):

$$K = \frac{1}{6} \kappa u_* D,$$

where  $\kappa = 0.4$  is von Karman's constant,  $u_* = \sqrt{C_d} U$  is the friction velocity, related to the turbulent intensity within the ISW plume,  $C_d$  is the basal drag coefficient,  $U = \sqrt{(U_p + U_a)^2 + (V_p + V_a)^2 + U_t^2}$  is the total flow speed,  $U_p(U_a)$  and  $V_p(V_a)$  are the depth-averaged ISW plume (ambient current) speed in the  $x$  and  $y$  directions respectively,  $U_t$  is the root-mean square tidal speed. Using a zero net flux condition in the equilibrium state at the lower boundary of the plume, i.e.,

$$\frac{K}{D} \frac{dc_i}{d\sigma} + w_i c_i = 0, \text{ for } \sigma=1$$

and a Dirichlet boundary condition at the upper boundary, i.e.,

$$c_i = c_{i,b}, \text{ for } \sigma=0$$

where  $c_{i,b}$  is the frazil concentration at the ice shelf/sea ice base, the vertical exponential profile for the equilibrium frazil concentration can be readily obtained (Cheng et al., 2017):

$$\frac{c_i(\sigma)}{c_{i,b}} = \exp(-6Z_*\sigma),$$

where  $Z_* = w_i / \kappa u_*$  is the suspension index, otherwise known as the Rouse number. Integrating this exponential profile from  $\sigma=0$  to 1, we finally obtain the relation between  $c_i(\sigma)$  and  $C_i$  as

$$\frac{c_i(\sigma)}{C_i} = \frac{6Z_* \exp(-6Z_*\sigma)}{1 - \exp(-6Z_*)}. \quad (2)$$

As shown in Fig. 2a, the vertical distribution of frazil concentration is strongly controlled by  $Z_*$ . The gradient of the vertical distribution becomes greater with increasing  $Z_*$ , and a vertically-uniform frazil concentration distribution can only be achieved as  $Z_*$  approaches 0. Accordingly, Cheng et al. (2017) introduced (2) into (1), and as a result significantly improved the simulated pattern of marine ice growth under the western side of Ronne Ice Shelf, compared with the VU and satellite-derived (Joughin and Padman, 2003) results. Hereinafter, we refer to this vertically-modified ISW plume model as VM. To conclude, the only difference between VM and VU models is whether the vertical distribution of frazil ice concentration is introduced.

30



The dependence of the integral value of  $I_{gr}$  on  $Z_*$  under specified conditions of supercooling (Fig. 2a) is shown in Fig. 2b, where  $D_{SC} = 50$  m (a value within the calculated range for the standard run, Fig. 1) in all the cases. It can be seen that the integral value increases nonlinearly with  $Z_*$ . The critical  $Z_*$  that represents the transition from frazil ice melting ( $I_{gr} < 0$ ) to freezing ( $I_{gr} > 0$ ) decreases as the supercooled part of ISW plume increases. In contrast, owing to the neglect of vertical variation in  $c_i$ , the integral values calculated using the VU formulation are constant, leading to transitions from overestimation of frazil ice growth to underestimation, compared with VM, as  $Z_*$  increases. Only if the ISW plume is fully supercooled ( $\sigma_{SC} = 1$ ) and  $Z_*$  is close to 0 are the integral values of  $I_{gr}$  calculated by VU and VM formulations equal (star in Fig. 2b). These features are illustrated in Fig. 2a: for given supercooling, if  $Z_*$  becomes larger, there is higher (lower) frazil concentration in the upper (lower), supercooled (overheated) part of the ISW plume. Owing to the assumption that thermohaline exchanges between frazil crystals and ambient water occur only at the crystal edge for freezing, but over the whole crystal surface for melting (Jenkins and Bombosch, 1995), the integral values of  $I_{gr}$  for the lower overheated part can be of much greater magnitude (Fig. 2b). It is therefore necessary to limit the mass loss due to frazil melting in one model time step such that it does not exceed the frazil concentration in the lower, overheated part of the plume. Overall, the frazil concentration and frazil growth rate distributions in the VM model show physically-reasonable and desirable characteristics that are absent from the VU model, and the impacts will be demonstrated by evaluation of the VM model in McMurdo Sound.

### 3 ISW model in McMurdo Sound

The unsteady VM and VU models used in this study are described in detail by Cheng et al. (2017). The governing equations for ISW properties and frazil concentration in both VM and VU models remain as they were in the depth-integrated, two-dimensional ISW plume model developed by Holland and Feltham (2006), except for the different treatments of the specific terms associated with the frazil ice growth rate, described above, in the frazil concentration and potential temperature transport equations of the VM model. Both VM and VU models combine the same commonly-used parameterizations of thermohaline exchanges across the ice–water interfaces, specifically a three-equation formulation (Holland and Jenkins, 1999) for the sea ice base and a two-equation formulation for frazil ice (Galton-Fenzi et al., 2012), with a multiple size–class frazil dynamics model (Smedsrud and Jenkins, 2004), to calculate basal freezing ( $f'$ ) and frazil melting/freezing ( $w'$ ), secondary nucleation ( $N'$ ), and precipitation ( $p'$ ). These processes are summarized in Fig. 3. Rather than repeat all the equations here, we recall some of them and present how we set up our ISW plume models on the McMurdo Sound domain.

The model domain (Fig. 1) is delimited by a 45×40 km rectangle in the  $x$ - $y$  plane with an ISW outflow from beneath McMurdo Ice Shelf. The base of the sea ice in McMurdo Sound is assumed to be horizontal and rough, owing to the presence of the platelet layer. The drag coefficient of the ice underside is therefore 6-30 times larger than that typically

applied in ice-ocean interaction models (Robinson et al, 2017). The parameterization of the sea ice thermodynamics, the assumption of no entrainment of ambient water into the ISW plume, and the boundary conditions at the ISW outflow follow HU14. The initial thickness of the ISW outflow from underneath McMurdo Ice Shelf is set equal to that of the supercooled layer, i.e.,  $D = D_{SC}$ , and the discharge per unit width is set to  $0.02 \text{ m}^2 \text{ s}^{-1}$ . The addition of both an ambient circulation and tides follow HU14: the former, which represented the only source of momentum in the study of HU14, is assumed to be parallel to the Victoria Land coast, in the negative  $y$  direction, and to be constant throughout the model domain; the latter is calculated using root-mean square tidal speeds from Padman and Erofeeva (2005). Because ISW persists in McMurdo Sound for at least the 8-9 months of the ice growth season (Robinson et al., 2014), all runs are integrated for 240 days. The model resolution and time step ( $\Delta t$ ) are 1 km and 25 s, respectively. The frazil ice size distribution is represented by 5 crystal size classes, and the transfer processes, induced by frazil freezing and melting, between different size classes are calculated using the scheme proposed by Smedsrud and Jenkins (2004). The ice concentration at the ISW outflow is evenly distributed among the classes (Holland and Feltham, 2005, 2006; Smedsrud and Jenkins, 2004).

We treat the frazil ice precipitation rate  $p'$  as inverted sedimentation and follow the parameterization of McCave and Swift (1976):

$$p' = w_i C_i \left(1 - \frac{U^2}{U_c^2}\right) \times He \left(1 - \frac{U^2}{U_c^2}\right), \quad (3)$$

where  $U_c$  is a critical velocity, above which precipitation cannot occur, determined by Jenkins and Bombosch (1995):

$$U_c^2 = \frac{\theta_i(\rho_0 - \rho_i)g^2 r_e}{\rho_0 C_D},$$

where  $\theta_i$  is the Shields criterion,  $\rho_0$  and  $\rho_i$  are reference seawater and ice densities, respectively,  $g$  is gravity,  $r_e$  is the equivalent radius of a sphere with the same volume as the frazil disk. The frazil ice rise velocity,  $w_i$ , is calculated by Morse and Richard (2009):

$$w_i = \begin{cases} 2.025D_i^{1.621} & \text{if } D_i \leq 1.27 \text{ mm} \\ -0.103D_i^2 + 4.069D_i - 2.024 & \text{if } 1.27 < D_i \leq 7 \text{ mm} \end{cases}$$

where  $D_i = 2r_i$  is the diameter of a frazil crystal in mm. The inclusion of the Heaviside function  $He$  means that negative precipitation (i.e., erosion of previously deposited frazil ice) is not permitted. Because we have no idea about how cohesive the ice crystals are once they have settled, the estimation of an erosion rate would entail additional uncertainties.

The complex processes after the frazil ice precipitates onto the sea ice base are simplified in our model. In order to calculate platelet layer thickness  $D_p$  at the  $n^{\text{th}}$  time interval, we adopt the assumptions of HU14 that solid ice fraction within the platelet layer in McMurdo Sound is 0.25 based on the observational estimation from Gough et al. (2012) and that the ice crystals, on average, double in volume after precipitation:

$$D_p = \frac{1}{0.25} \times 2 \times \sum_{k=1}^n (p'_k \times \Delta t).$$

It should be noted that the volume change factor is a broad estimate, with almost no supporting evidence in the literature to guide it.

## 4 Results

### 4.1 Standard model run

5 The performance of the VU and VM models in reproducing the ISW supercooling and platelet layer pattern in McMurdo Sound is evaluated by comparing results with observational data. To our knowledge, the data reported by HU14 are the most comprehensive available to evaluate our model, including both oceanographic and ice core data in two horizontal dimensions adjacent to McMurdo Ice Shelf. As this study represents the first application of a two-dimensional ISW plume model to the McMurdo Sound region, extensive tuning of the least constrained model parameters, including the ISW outflow properties, 10 platelet layer basal drag coefficient, frazil ice crystal size distribution, ambient current speed, and Shields criterion was required to produce the distributions of ISW properties and platelet layer thickness shown in Figs. 4a and 6, respectively. Table 1 gives values adopted for the key parameters. Model results are evaluated by means of skill metrics: Root-Mean-Square Error (RMSE), Correlation Coefficient (CC), and Skill Score (SS), respectively given by

$$RMSE = \left[ \frac{\sum (X_{cal} - X_{obs})^2}{M} \right]^{1/2},$$

$$15 \quad CC = \frac{\sum (X_{cal} - \bar{X}_{cal})(X_{obs} - \bar{X}_{obs})}{[\sum (X_{cal} - \bar{X}_{cal})^2 \sum (X_{obs} - \bar{X}_{obs})^2]^{1/2}},$$

$$SS = 1 - \frac{\sum (X_{cal} - X_{obs})^2}{\sum (X_{obs} - \bar{X}_{obs})^2},$$

where  $X$  is the variable being evaluated,  $M$  is the number of data points, and the overbar denotes the arithmetic mean. The performance of each model is indicated by SS as:  $>0.65$  excellent;  $0.65-0.5$  very good;  $0.5-0.2$  good;  $<0.2$  poor (Luo et al., 2017; Ralston et al., 2010; Song and Wang, 2013).

20

It can be seen that at the end of the simulations both VM and VU models reproduce the observed reduction in ISW supercooling at the sea ice base ( $T_{SC}^0$ , superscript “0” denotes the sea ice base) in the cross- and long-sound directions, in spite of some evident model discrepancies (Fig. 4a) that may result from the limitations in our model setup: both the ambient current and tides are treated as temporally and spatially constant; there are no long-term observations of ISW outflow to provide reliable boundary conditions; we use a constant drag coefficient, ignoring the spatiotemporal evolution of the sea ice basal form characterized by the platelet layer. Nevertheless, the SS of  $T_{SC}^0$  calculated using VM and VU models are 0.56 and 0.58, respectively, and the CC and RMSE are also reasonable (Table 2). There are only small differences throughout the time series of  $T_{SC}^0$  simulated by the VM and VU models (Fig. 4) and the final distributions of both total ISW plume thickness and supercooled thickness are also very similar (see Fig. 5a-d). A comprehensive comparison of  $T_{SC}^0$  calculated by the VM and

VU models in an extensive set of sensitivity experiments will be discussed later. Finally, it can be seen that in both models the ISW plume flow is predominantly governed by a geostrophic balance (Fig 5a-d).

In contrast, the frazil concentration (red lines in Fig. 4b, Fig. 5e and f) and platelet layer thickness (green lines in Fig. 4b, Fig. 6b and c) are both underestimated by the VU model, compared with the results of the VM model, throughout the time series. Given the small differences in  $T_{SC}^0$  calculated by VM and VU models, this result demonstrates that the vertical distribution of frazil concentration within the ISW plume plays a critical role in determining the suspended frazil ice growth (Fig. 2), and thus the frazil concentration and platelet layer thickness distributions. The supercooling is utilized more efficiently in the VM model, giving a greater depth-averaged frazil concentration than is produced by the commonly-used VU model. Because the sea ice base is horizontal, there are no changes in the freezing point associated with pressure change, so supercooling is always highest at the ISW outflow (Fig. 5c and d). That results in the greatest frazil concentration (Fig. 5f) and platelet layer thickness (Fig. 6b) near the location of the outflow, with large changes from  $2.2 \times 10^{-4}$  to  $4 \times 10^{-5}$  and 15 to 6 m, respectively, in the case of the VM model within 5 km of the outflow. Such small-scale features in the platelet layer thickness distribution, if present, were not resolved by the relatively coarse spatial distribution of ice-core sampling (dots in Fig. 6). Nevertheless, the platelet layer thickness calculated by the VM model at drill sites agrees well with the measurements (Fig. 6a), being graded “excellent” in contrast with the “poor” performance of the VU model (Table 2). Despite efforts to tune the VU model to give a better match with the observed platelet layer thickness, even a limited expansion of the platelet layer can only be achieved with a considerable increase in the calculated  $T_{SC}^0$ , in disagreement with the observations.

For both VM and VU models, the time series of area-averaged  $T_{SC}^0$ ,  $C_i$  (hereafter  $T_{SC}^0$  and  $C_i$  denote their area-average values), and platelet layer thickness indicate respectively two near-constant values and one near-constant growth rate after about the 150<sup>th</sup> day (Fig. 4b). It is informative to explore how our various assumptions about the vertical distribution of frazil concentration influence the steady-state relationship between those variables in the McMurdo Sound region.

#### 4.2 Dependence of platelet layer thickening rate on ISW supercooling

The response of ice shelf basal melting to variations in ocean temperature has been investigated using satellite altimetry (Rignot and Jacobs, 2002; Shepherd et al., 2004) and numerical models (Grosfeld and Sandhäger, 2004; Holland et al., 2008; Payne et al., 2007; Walker and Holland, 2007; Williams et al., 1998, 2002). In contrast, we know of no studies to date of the response of marine ice (or platelet layer) thickening rate beneath ice shelves (or sea ice) to variations in supercooling, which is of potential significance for evaluating the mass balance of deep-draughting ice shelves in cold water environments and adjacent sea ice subject to climatic variability.

Owing to the number of poorly-constrained parameters in the frazil-ice-laden ISW plume model, we conducted 211 comparative sensitivity experiments between VM and VU models, varying both physical and input parameters, including

drag coefficient, frazil ice crystal size configuration, average number of frazil crystals, ambient current speed, width and thickness of the ISW outflow, and frazil concentration within the outflow (see Table 3). For all model runs, we plot the relationship between  $T_{SC}^0$  and thickening rate in the steady state, using output from the last 30 days of each run (Fig. 7).

- 5 In Fig. 7a, the results of the VM model are grouped by the prescribed supercooled layer thickness  $D_{SC}^{ini}$  in the ISW outflow. For  $D_{SC}^{ini} < 65$  m there is a relatively consistent increase in thickening rate with increasing  $T_{SC}^0$ , while for  $D_{SC}^{ini} \geq 65$  m the thickening rate tends to be much more variable. It is worth mentioning that  $D_{SC}^{ini} = 65$  m is the value estimated by HU14 based on the measurements conducted by Lewis and Perkin (1985) and Jones and Hill (2001). For  $D_{SC}^{ini} = 78$  m and greater, inflexions emerge separating a region of low thickening rate, where the thickening rate tends to decrease with increasing  $T_{SC}^0$ ,  
 10 from a region of high thickening rate, where there is a very rapid increase in thickening rate with increasing  $T_{SC}^0$ . This complex response of the VM model must result from the consideration of vertical structure in the frazil concentration, controlled by the frazil ice suspension index  $Z_*$  (Fig. 2), in the calculation of frazil ice growth.

We therefore calculated the weighted-average of  $Z_*$  at each grid point for the VM model using the following equation:

15 
$$\bar{Z}_* = \frac{\sum_{k=1}^n C_i^k Z_*^k}{\sum_{k=1}^n C_i^k} = \frac{\sum_{k=1}^n C_i^k Z_*^k}{C_i},$$

- where  $C_i^k$  is the frazil concentration of the  $k^{\text{th}}$  size class, and  $n$  is the number of size classes used. Then, we took the average of  $\bar{Z}_*$  over all the grid points occupied by the plume to give a representative suspension index for the VM runs (hereinafter  $\bar{Z}_*$  denotes its area-averaged value). We replotted the VM model results characterized by  $\bar{Z}_*$  in Fig. 7b. We find systematic changes in  $\bar{Z}_*$  with increasing thickening rate (along the coloured lines in Fig. 7b), particularly for  $D_{SC}^{ini} \geq 78$  m where the  
 20 inflexions emerge. With decreasing  $\bar{Z}_*$ ,  $T_{SC}^0$  first decreases, and then increases. If  $\bar{Z}_*$  is sufficiently large, the suspended frazil crystals deposit out of the ISW plume so rapidly that they cannot efficiently use the ISW supercooling to grow, leading to the smallest platelet layer production for the VM model. For smaller  $\bar{Z}_*$ , the frazil crystals bathed in the supercooled layer of the ISW plume can remain in suspension and grow longer, resulting in a thicker platelet layer and less residual supercooling. However, if  $\bar{Z}_*$  decreases further, higher frazil concentration occurs within the lower, overheated part of the ISW plume,  
 25 where melting of the crystals can mitigate the release of latent heat (Fig. 2b). That promotes further growth of frazil ice which can remain in suspension even longer, and thus lead to rapid platelet layer production. The thickening rate calculated by the VU model is also shown, and is discernibly smaller than that calculated by the VM model. In addition, the maximum values of  $T_{SC}^0$  were obtained within the VU model, because the supercooling is used less efficiently for producing the platelet layer in the VU than in the corresponding VM runs.

30

These arguments can be further illustrated by a more detailed comparison of  $T_{SC}^0$  calculated by the VM and VU models (Fig. 8). There are a number of runs, including the standard run, that have larger  $T_{SC}^0$  values in the VM than in the VU model. The trend from larger  $T_{SC}^0$  in the VM model to larger  $T_{SC}^0$  in the VU model is accompanied by increases in  $\bar{Z}_*$ . When  $\bar{Z}_*$  is relatively small, large frazil concentration exists within the lower overheated part of the ISW plume (Fig. 2b) where melting of frazil ice (causing cooling) counteracts the consumption of supercooling by frazil growth (causing warming) in the upper part of the plume. As  $\bar{Z}_*$  increases, the frazil concentration within the lower overheated part decreases, and finally vanishes, and the resulting release of supercooling in the upper part is more efficient in the VM model, giving larger  $T_{SC}^0$  values in the VU model.

10 In Fig. 7a, when  $D_{SC}^{ini} < 65$  m, ISW supercooling is insufficient to distinguish runs with different  $\bar{Z}_*$ . In other words, the relation between thickening rate and  $T_{SC}^0$  is independent of  $\bar{Z}_*$  for such small  $D_{SC}^{ini}$ . When  $D_{SC}^{ini}$  is within the range of 65 to 78 m, the VM model results are distinguishable, with data points having smaller thickening rate and larger  $T_{SC}^0$  corresponding to larger  $\bar{Z}_*$  (Fig. 7b). When  $D_{SC}^{ini} \geq 78$  m, the inflexions emerge, and the ISW supercooling revives when  $\bar{Z}_*$  decreases further. Therefore, we conclude that when  $D_{SC}^{ini}$  exceeds a critical value (about 65 m for these McMurdo Sound simulations), the efficiency of converting ISW supercooling into frazil ice growth is controlled by the suspension index.

### 4.3 Dependence of frazil concentration on ISW supercooling

In view of the correlation between platelet layer thickening rate and frazil concentration shown in Eq. (3) (also see Fig. 5e and f; Fig. 6b and c), we will explore the relationship between  $T_{SC}^0$  and  $C_i$  here. As expected, the complex response of  $C_i$  to variations in  $T_{SC}^0$  (Fig. 9) is similar to the relationship between  $T_{SC}^0$  and thickening rate (Fig. 7) in the VM model.

20

The magnitude of the difference in  $C_i$  calculated by VM and VU models (VM minus VU) is compared in Fig. 10a, where we find that  $C_i$  calculated by the VM model is always larger than that calculated by the VU model. In general, the difference increases with decreasing  $\bar{Z}_*$ , while the sensitivity grows with increasing  $D_{SC}^{ini}$ . The dependence on  $\bar{Z}_*$  is once again due to the impact of the combined thermodynamic processes, i.e., the efficient growth in the upper supercooled part of the plume together with the maintenance of supercooling by melting of frazil in the lower part, discussed above. We also see similar behavior for the difference in the thickening rate (Fig. 10b).

Fig. 7 (Fig. 9) suggests a possible relationship between platelet layer thickening rate (frazil concentration) and supercooling in McMurdo Sound, but observations of suspended frazil ice crystal sizes and turbulence within the ISW would be needed to calculate a representative suspension index. To date, there are limited observations of frazil ice in situ, and the majority of the observations made use of instruments not specifically designed for ice crystal detection (Leonard et al., 2006).

30

## 5 Summary and future works

In this study, we demonstrated how the vertical distributions of supercooling and frazil ice concentration within an ISW plume jointly determine the growth of suspended frazil ice, and thus the rate of platelet layer formation [under sea ice and marine ice beneath ice shelves](#). A vertically-modified, frazil-ice-laden, ISW plume model which encapsulates these combined nonlinear effects was applied to the McMurdo Sound region, and reproduced the observed ISW supercooling and platelet layer distributions in two horizontal dimensions. Using multiple model runs, the relationship of ISW supercooling to platelet layer thickening rate and frazil concentration in McMurdo Sound was explored, [and shown to be dependent](#) on the suspension index that controls the vertical distribution of frazil concentration within the ISW plume. Moreover, when the thickness of a supercooled layer of ISW is large enough, the efficiency of converting ISW supercooling into frazil concentration, and thus platelet layer growth is determined by the suspension index. [These findings highlight the need for further](#) observations in McMurdo Sound, particularly focused near the ISW outflow region in the western sound, where the supercooled ISW plume and platelet layer are prominent, and more general observations that help to constrain the frazil size spectrum within the sea ice-ocean boundary layer. [In addition](#), the performance of the VM model in providing reliable estimates of supercooling and frazil ice flux at the platelet layer base makes it an attractive tool for coupling with sea ice models focusing on microscale processes within the bottom layer of the ice (Buffo et al., 2018).

It would be straightforward for the next step to investigate the relationship between supercooling and marine ice thickening rate underneath ice shelves using the VM model. Quantifying this relationship would be the key to parameterizing the process in more complex three-dimensional, primitive equation ocean models, which frequently neglect details of the ice shelf-ocean boundary layer and processes associated with an evolving suspension of frazil ice crystals (Liu et al., 2017; Mueller et al., 2012, 2018). The main difference between the process of marine ice accretion beneath ice shelves and the growth of the sub-ice platelet layer discussed here is likely to be the magnitude of the vertical heat flux that the deposited frazil ice is subjected to. At the base of an ice shelf, typically several hundred meters thick, the vertical temperature gradient is comparatively small, so the deposited crystals form a slushy layer (Engelhardt and Determann, 1987) that slowly consolidates, possibly as much through compaction as freezing. The ice-ocean interface and the associated drag coefficient are therefore likely to be very different to those observed in McMurdo Sound, where the platelet layer appears to comprise a more open matrix of ice and water that consolidates by freezing as heat is lost to the atmosphere. Therefore, the VM model would need to be re-evaluated against observations of sub-ice shelf ISW plumes and the ice shelf-ocean boundary layer. [Finally](#), further process studies, including the influence of the vertical current structure within [either the ice shelf or sea ice - ocean boundary layer](#) (Jenkins, 2016; [Robinson et al., 2017](#)) could also contribute to improving our understanding of marine ice and platelet layer formation.

*Data availability.* The data archive associated with this study can be found in the Global Change Master Directory under the keyword K063\_2011\_2012\_NZ\_1.

*Author contributions.* CC led the study. The simulations were designed by ZW and CC, implemented by CL and RX, and analyzed by CC, AJ, and PRH. The paper was written by CC, AJ, and PRH.

5 *Competing interests.* The authors declare that they have no conflict of interest.

*Acknowledgements.* We would like to thank two anonymous referees and Ken Hughes for their thorough review and helpful comments and suggestions. This work was funded by the National Natural Science Foundation of China (41406214, 41306208, 41606217). CC and CL were respectively supported by the China Scholarship Council (201708320046, 201504180026). ZW was supported by “the Fundamental Research Funds for the Central Universities” (2017B04814, 2017B20714).

## References

- Arrigo, K. R., Mock, T., and Lizotte, M. P.: Primary producers and sea ice, *Sea ice*, 2, 283-325, 2010.
- Bombosch, A. and Jenkins, A.: Modeling the formation and deposition of frazil ice beneath Filchner-Ronne Ice Shelf, *J. Geophys. Res.-Oceans*, 100, 6983-6992, <http://doi.org/10.1029/94JC03224>, 1995.
- 15 Buffo, J. J., Schmidt, B. E., and Huber, C.: Multiphase Reactive Transport and Platelet Ice Accretion in the Sea Ice of McMurdo Sound, Antarctica, *J. Geophys. Res.-Oceans*, 123, 324-345, <https://doi.org/10.1002/2017JC013345>, 2018.
- Cheng, C., Song, Z. Y., Wang, Y. G., and Zhang, J. S.: Parameterized expressions for an improved Rouse equation, *Int. J. Sediment Res.*, 28, 523-534, [http://doi.org/10.1016/S1001-6279\(14\)60010-X](http://doi.org/10.1016/S1001-6279(14)60010-X), 2013.
- Cheng, C., Huang, H., Liu, C., and Jiang, W.: Challenges to the representation of suspended sediment transfer using a depth-averaged flux, *Earth Surf. Proc. Land*, 41, 1337-1357, <http://doi.org/10.1002/esp.3903>, 2016.
- 20 Cheng, C., Wang, Z., Liu, C., and Xia, R.: Vertical Modification on Depth-Integrated Ice Shelf Water Plume Modeling Based on an Equilibrium Vertical Profile of Suspended Frazil Ice Concentration, *J. Phys. Oceanogr.*, 47, 2773-2792, <http://doi.org/10.1175/JPO-D-17-0092.1>, 2017.
- Dempsey, D. E., Langhorne, P. J., Robinson, N. J., Williams, M. J. M., Haskell, T. G., and Frew, R. D.: Observation and modeling of platelet ice fabric in McMurdo Sound, Antarctica, *J. Geophys. Res.-Oceans*, 115, <https://doi.org/10.1029/2008JC005264>, 2010.
- 25 [Engelhardt, H. and Determann, J.: Borehole evidence for a thick layer of basal ice in the central Ronne Ice Shelf, \*Nature\*, 327, 318–319, https://doi.org/10.1038/327318a0, 1987.](https://doi.org/10.1038/327318a0)
- Fricke, H. A., Popov, S., Allison, I., and Young, N.: Distribution of marine ice beneath the Amery Ice Shelf, *Geophys. Res. Lett.*, 28, 2241-2244, <https://doi.org/10.1029/2000GL012461>, 2001.
- 30



- Galton-Fenzi, B. K., Hunter, J. R., Coleman, R., Marsland, S. J., and Warner, R. C.: Modeling the basal melting and marine ice accretion of the Amery Ice Shelf, *J. Geophys. Res.-Oceans*, 117, <http://doi.org/10.1029/2012JC008214>, 2012.
- Gough, A. J., Mahoney, A. R., Langhorne, P. J., Williams, M. J., Robinson, N. J., and Haskell, T. G.: Signatures of supercooling: McMurdo Sound platelet ice, *J. Glaciol.*, 58, 38-50, <https://doi.org/10.3189/2012JoG10J218>, 2012.
- 5 Grosfeld, K. and Sandhäger, H.: The evolution of a coupled ice shelf–ocean system under different climate states, *Global Planet. Change*, 42, 107-132, <http://doi.org/10.1016/j.gloplacha.2003.11.004>, 2004.
- Herraiz-Borreguero, L., Allison, I., Craven, M., Nicholls, K. W., and Rosenberg, M. A.: Ice shelf/ocean interactions under the Amery Ice Shelf: Seasonal variability and its effect on marine ice formation, *J. Geophys. Res.-Oceans*, 118, 7117-7131, <https://doi.org/10.1002/2013JC009158>, 2013.
- 10 Holland, P. R. and Feltham, D. L.: Frazil dynamics and precipitation in a water column with depth-dependent supercooling, *J. Fluid Mech.*, 530, 101-124, <https://doi.org/10.1017/S002211200400285X>, 2005.
- Holland, P. R. and Feltham, D. L.: The effects of rotation and ice shelf topography on frazil-laden ice shelf water plumes, *J. Phys. Oceanogr.*, 36, 2312-2327, <https://doi.org/10.1175/JPO2970.1>, 2006.
- Holland, P. R., Feltham, D. L., and Jenkins, A.: Ice shelf water plume flow beneath Filchner-Ronne Ice Shelf, Antarctica, *J. Geophys. Res.-Oceans*, 112, <https://doi.org/10.1029/2006JC003915>, 2007.
- 15 Holland, P. R., Jenkins, A., and Holland, D. M.: The response of ice shelf basal melting to variations in ocean temperature, *J. Climate*, 21, 2558-2572, <https://doi.org/10.1175/2007JCLI1909.1>, 2008.
- Holland, P. R., Corr, H. F., Vaughan, D. G., Jenkins, A., and Skvarca, P.: Marine ice in Larsen ice shelf, *Geophys. Res. Lett.*, 36, <https://doi.org/10.1029/2009GL038162>, 2009.
- 20 Hughes, K. G., Langhorne, P. J., Leonard, G. H., and Stevens, C. L.: Extension of an Ice Shelf Water plume model beneath sea ice with application in McMurdo Sound, Antarctica, *J. Geophys. Res.-Oceans*, 119, 8662-8687, <https://doi.org/10.1002/2013JC009411>, 2014.
- Hunkeler, P. A., Hoppmann, M., Hendricks, S., Kalscheuer, T., and Gerdes, R.: A glimpse beneath Antarctic sea ice: Platelet layer volume from multifrequency electromagnetic induction sounding, *Geophys. Res. Lett.*, 43, 222-231, <https://doi.org/10.1002/2015GL065074>, 2016.
- 25 Jenkins, A.: A simple model of the ice shelf–ocean boundary layer and current, *J. Phys. Oceanogr.*, 46, 1785-1803, <http://doi.org/10.1175/JPO-D-15-0194.1>, 2016.
- Jenkins, A. and Bombosch, A.: Modeling the effects of frazil ice crystals on the dynamics and thermodynamics of ice shelf water plumes, *J. Geophys. Res.-Oceans*, 100, 6967-6981, <http://doi.org/10.1029/94JC03227>, 1995.
- 30 Jones, S. J. and Hill, B. T.: Structure of sea ice in McMurdo Sound, Antarctica, *Ann. Glaciol.*, 33, 5-12, <http://doi.org/10.3189/172756401781818347>, 2001.
- Joughin, I. and Padman, L.: Melting and freezing beneath Filchner-Ronne Ice Shelf, Antarctica, *Geophys. Res. Lett.*, 30, <http://doi.org/10.1029/2003GL016941>, 2003.

- Langhorne, P. J., Hughes, K. G., Gough, A. J., Smith, I. J., Williams, M. J. M., Robinson, N. J., Stevens, C. L., Rack, W., Price, D., Leonard, G. H., Mahoney, A. R., Haas, C., Haskell, T. G.: Observed platelet ice distributions in Antarctic sea ice: An index for ocean-ice shelf heat flux, *Geophys. Res. Lett.*, 42, 5442-5451, <https://doi.org/10.1002/2015GL064508>, 2015.
- 5 Lewis, E. L. and Perkin, R. G.: The winter oceanography of McMurdo Sound, Antarctica, *Oceanology of the Antarctic continental shelf*, 145-165, <https://doi.org/10.1029/AR043p0145>, 1985.
- Leonard, G. H., Purdie, C. R., Langhorne, P. J., Haskell, T. G., Williams, M. J. M., and Frew, R. D.: Observations of platelet ice growth and oceanographic conditions during the winter of 2003 in McMurdo Sound, Antarctica, *J. Geophys. Res.-Oceans*, 111, <https://doi.org/10.1029/2005JC002952>, 2006.
- 10 Liu, C., Wang, Z., Cheng, C., Xia, R., Li, B., and Xie, Z.: Modeling modified Circumpolar Deep Water intrusions onto the Prydz Bay continental shelf, East Antarctica, *J. Geophys. Res.-Oceans*, 122, 5198-5217, <http://doi.org/10.1002/2016JC012336>, 2017.
- Luo, Z., Zhu, J., Wu, H., and Li, X.: Dynamics of the sediment plume over the Yangtze Bank in the Yellow and East China Seas, *J. Geophys. Res.-Oceans*, 122, 10073-10090, <https://doi.org/10.1002/2017JC013215>, 2017.
- 15 McCave, I. N. and Swift, S. A.: A physical model for the rate of deposition of fine-grained sediments in the deep sea, *Geological Society of America Bulletin*, 87, 541-546, [https://doi.org/10.1130/0016-7606\(1976\)87<541:APMFTR>2.0.CO;2](https://doi.org/10.1130/0016-7606(1976)87<541:APMFTR>2.0.CO;2), 1976.
- Morgan, V. I.: Oxygen isotope evidence for bottom freezing on the Amery Ice Shelf, *Nature*, 238, 393, <https://doi.org/10.1038/238393a0>, 1972.
- 20 Morse, B. and Richard, M.: A field study of suspended frazil ice particles, *Cold Reg. Sci. Technol.*, 55, 86-102, <https://doi.org/10.1016/j.coldregions.2008.03.004>, 2009.
- Mueller, R. D., Hattermann, T., Howard, S. L., and Padman, L.: Tidal influences on a future evolution of the Filchner–Ronne Ice Shelf cavity in the Weddell Sea, Antarctica, *The Cryosphere*, 12, 453, <http://doi.org/10.5194/tc-12-453-2018>, 2018.
- Mueller, R. D., Padman, L., Dinniman, M. S., Erofeeva, S. Y., Fricker, H. A., and King, M. A.: (2012), Impact of tide-topography interactions on basal melting of Larsen C Ice Shelf, Antarctica, *J. Geophys. Res.-Oceans*, 117, C05005, <https://doi.org/10.1029/2011JC007263>, 2012.
- 25 Oerter, H., Kipfstuhl, J., Determann, J., Miller, H., Wagenbach, D., Minikin, A., and Graft, W.: Evidence for basal marine ice in the Filchner–Ronne Ice Shelf, *Nature*, 358, 399, <https://doi.org/10.1038/358399a0>, 1992.
- Padman, L. and Erofeeva, S.: Tide Model Driver (TMD) Manual, Version 1.2, Earth and Space Research, Seattle, Wash., 2005. [Available at [www.esr.org/polar\\_tide\\_models/README\\_TMD.pdf](http://www.esr.org/polar_tide_models/README_TMD.pdf), last accessed 7 Nov. 2012.]
- 30 Payne, A. J., Holland, P. R., Shepherd, A. P., Rutt, I. C., Jenkins, A., and Joughin, I.: Numerical modeling of ocean-ice interactions under Pine Island Bay's ice shelf, *J. Geophys. Res.-Oceans*, 112, <http://doi.org/10.1029/2006JC003733>, 2007.

- Ralston, D. K., Geyer, W. R., and Lerczak, J. A.: Structure, variability, and salt flux in a strongly forced salt wedge estuary, *J. Geophys. Res.-Oceans*, 115, C06005, <https://doi.org/10.1029/2009JC005806>, 2010.
- Rees Jones, D. W. and Wells, A. J.: Frazil-ice growth rate and dynamics in mixed layers and sub-ice-shelf plumes, *The Cryosphere*, 12, 25-38, <http://doi.org/10.5194/tc-12-25-2018>, 2018.
- 5 Rignot, E. and Jacobs, S. S.: Rapid bottom melting widespread near Antarctic ice sheet grounding lines, *Science*, 296, 2020-2023, <http://doi.org/10.1126/science.1070942>, 2002.
- Rignot, E., Jacobs, S., Mouginot, J., and Scheuchl, B.: Ice-shelf melting around Antarctica, *Science*, 341, 266-270, <https://doi.org/10.1126/science.1235798>, 2013.
- Robinson, N. J., Stevens, C. L., and McPhee, M. G.: Observations of amplified roughness from crystal accretion in the sub-ice ocean boundary layer, *Geophys. Res. Lett.*, 44, 1814-1822, <https://doi.org/10.1002/2016GL071491>, 2017.
- 10 Robinson, N. J., Williams, M. J., Stevens, C. L., Langhorne, P. J., and Haskell, T. G.: Evolution of a supercooled Ice Shelf Water plume with an actively growing subice platelet matrix, *J. Geophys. Res.-Oceans*, 119, 3425-3446, <https://doi.org/10.1002/2013JC009399>, 2014.
- Shepherd, A., Wingham, D., and Rignot, E.: Warm ocean is eroding West Antarctic ice sheet, *Geophys. Res. Lett.*, 31, <http://doi.org/10.1029/2004GL021106>, 2004.
- 15 Smedsrud, L. H. and Jenkins, A.: Frazil ice formation in an ice shelf water plume, *J. Geophys. Res.-Oceans*, 109, <http://doi.org/10.1029/2003JC001851>, 2004.
- Smith, I. J., Langhorne, P. J., Haskell, T. G., Trodahl, H. J., Frew, R., and Vennell, M. R.: Platelet ice and the land-fast sea ice of McMurdo Sound, Antarctica, *Ann. Glaciol.*, 33, 21-27, <http://doi.org/10.3189/172756401781818365>, 2001.
- 20 Song, D. and Wang, X. H.: Suspended sediment transport in the Deepwater Navigation Channel, Yangtze River Estuary, China, in the dry season 2009: 2. Numerical simulations, *J. Geophys. Res.-Oceans*, 118, 5568-5590, <http://doi.org/10.1002/jgrc.20411>, 2013.
- Stern, A. A., Dinniman, M. S., Zagorodnov, V., Tyler, S. W., and Holland, D. M.: Intrusion of warm surface water beneath the McMurdo Ice Shelf, Antarctica, *J. Geophys. Res.-Oceans*, 118, 7036-7048, <https://doi.org/10.1002/2013JC008842>, 25 2013.
- [Svensson, U. and Omstedt, A.: Numerical simulations of frazil ice dynamics in the upper layers of the ocean, \*Cold Reg. Sci. Technol.\*, 28, 29-44. \[http://doi.org/10.1016/S0165-232X\\(98\\)00011-1\]\(http://doi.org/10.1016/S0165-232X\(98\)00011-1\), 1998.](#)
- Walker, R. T. and Holland, D. M.: A two-dimensional coupled model for ice shelf–ocean interaction, *Ocean Model.*, 17, 123-139, <http://doi.org/10.1016/j.ocemod.2007.01.001>, 2007.
- 30 Williams, M. J. M., Warner, R. C., and Budd, W. F.: The effects of ocean warming on melting and ocean circulation under the Amery Ice Shelf, East Antarctica, *Ann. Glaciol.*, 27, 75-80, <http://doi.org/10.3189/1998AoG27-1-75-80>, 1998.
- Williams, M. J. M., Warner, R. C., and Budd, W. F.: Sensitivity of the Amery Ice Shelf, Antarctica, to changes in the climate of the Southern Ocean, *J. Climate*, 15, 2740-2757, [http://doi.org/10.1175/1520-0442\(2002\)015<2740:SOTAIS>2.0.CO;2](http://doi.org/10.1175/1520-0442(2002)015<2740:SOTAIS>2.0.CO;2), 2002.

**Table 1: List of parameters used in standard model run.**

Parameter	Value	Description
$f$	$-1.4244 \times 10^{-4} \text{ s}^{-1}$	Coriolis parameter
$D_{ini}(D_{SC}^{ini})$	78 m	Constant ISW plume outflow thickness (constant outflow supercooled layer thickness)
$W_{ini}$	3 km	ISW plume outflow width with constant $D_{ini}(D_{SC}^{ini})$
$C_t^{ini}$	$1 \times 10^{-6}$	Depth-averaged volumetric frazil concentration in outflow
$N_{ice}$	5	Number of frazil ice sizes
$r_{i,1}, r_{i,2}, r_{i,3}, r_{i,4}, r_{i,5}$	0.2, 0.6, 0.9, 1.2, 1.5 mm	Frazil ice radii for each class
$a_r$	0.02	Aspect ratio of frazil discs
$\bar{n}$	$1 \times 10^3 \text{ m}^{-3}$	Average number of frazil crystals in all size classes per unit volume
$C_d$	0.02	Platelet layer basal drag coefficient
$V_a$	$-0.01 \text{ m s}^{-1}$	Ambient flow speed
$A_H$	$100 \text{ m}^2 \text{ s}^{-1}$	Horizontal eddy viscosity
$K_H$	$20 \text{ m}^2 \text{ s}^{-1}$	Horizontal turbulent diffusivity
$S_{ini}$	34.59 psu	ISW plume outflow salinity
$T_{ini}$	$-0.0573 \times S_{ini} + 0.0832 - 7.61 \times 10^{-4} D_{ini}$	ISW plume outflow temperature
$\theta_i$	0.075	Shields criterion number

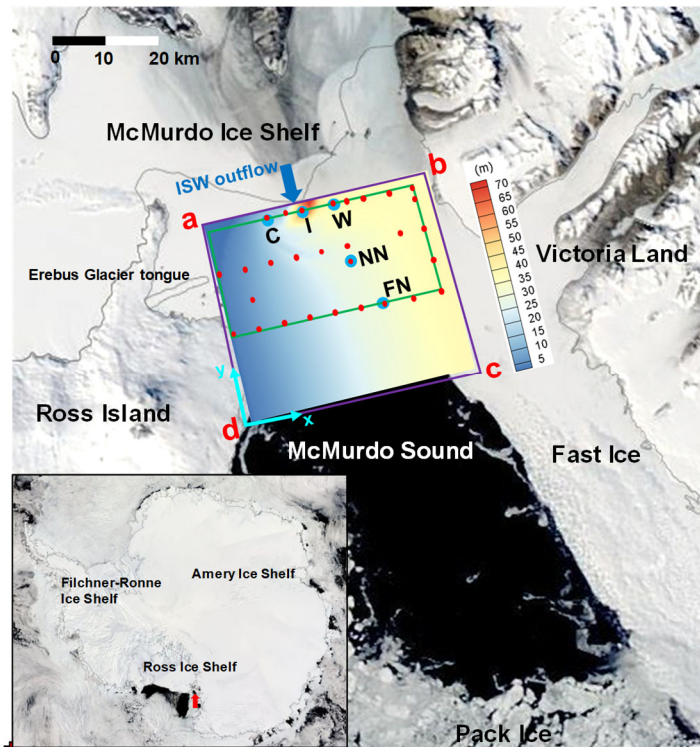
**Table 2: List of calculated skill metrics for the results of VM and VU standard model runs.**

Variable	RMSE		CC		SS	
	VM	VU	VM	VU	VM	VU
$T_{SC}^0$	0.0070 °C	0.0069 °C	0.83	0.84	0.56	0.58
Platelet layer thickness	1.034 m	2.928 m	0.91	0.01	0.79	-0.65

**Table 3: Parameter settings for sensitivity runs, indicated by check, colour-coded by ISW outflow thickness (bottom row). All other parameters remain as they were for the standard model run.**

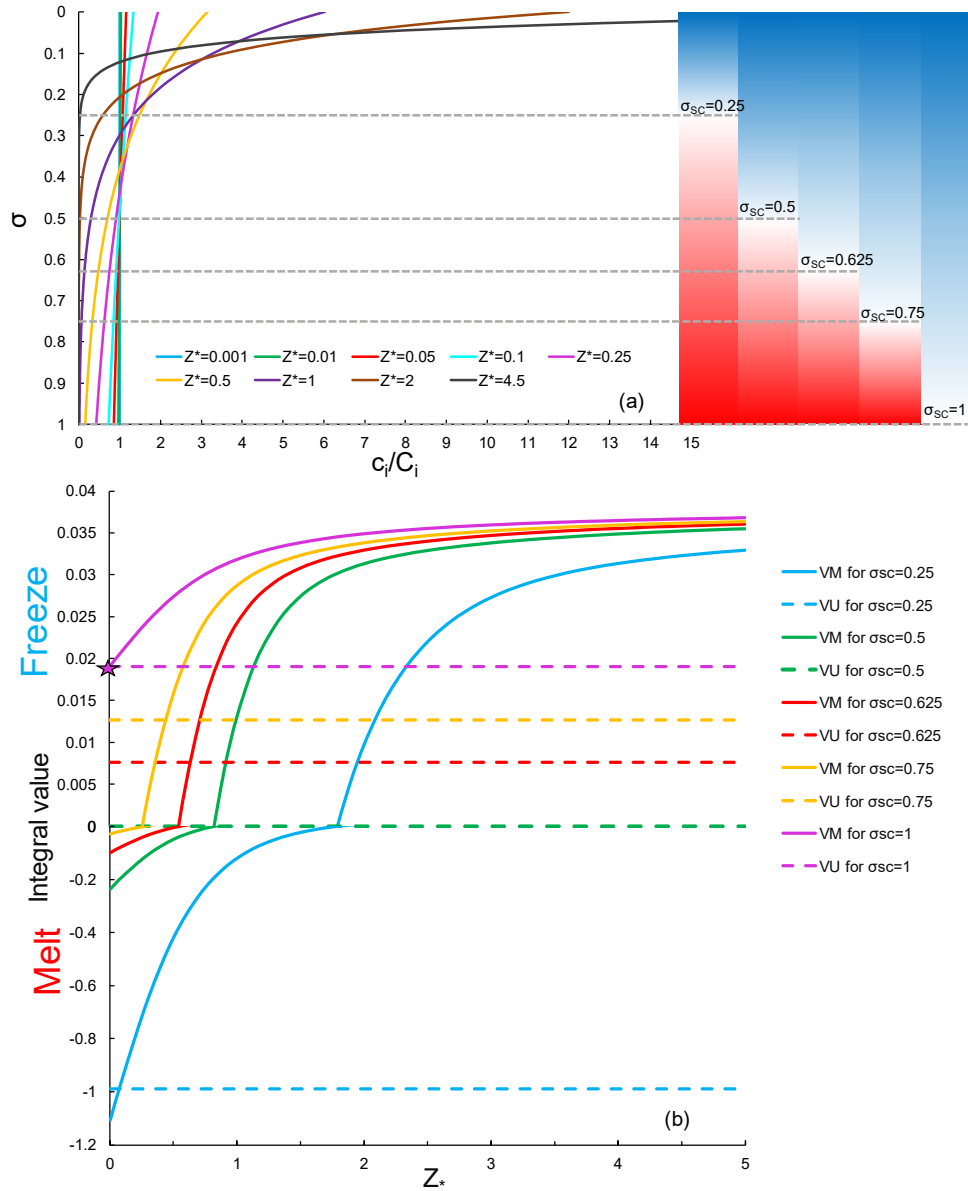
		Drag coefficient						
		0.015	0.0175	0.02	0.0225	0.025		
Frazil size configuration (mm)	A: (0.2,0.6,0.9,1.2,1.5)	✓✓✓✓✓✓✓✓		✓✓✓✓✓✓✓✓		✓✓✓✓✓✓✓✓		
	1.125×A		✓✓✓✓✓✓✓✓		✓✓✓✓✓✓✓✓			
	1.25×A		✓✓✓✓✓✓✓✓		✓✓✓✓✓✓✓✓			
	1.375×A		✓✓✓✓✓✓✓✓		✓✓✓✓✓✓✓✓			
	1.5×A	✓✓✓✓✓✓✓✓		✓✓✓✓✓✓✓✓		✓✓✓✓✓✓✓✓		
	1.625×A		✓✓✓✓✓✓✓✓		✓✓✓✓✓✓✓✓			
	1.75×A		✓✓✓✓✓✓✓✓		✓✓✓✓✓✓✓✓			
	1.875×A		✓✓✓✓✓✓✓✓		✓✓✓✓✓✓✓✓			
	2×A	✓✓✓✓✓✓✓✓		✓✓✓✓✓✓✓✓		✓✓✓✓✓✓✓✓		
	$W_{ini}$ -ISW plume outflow width with constant $D_{ini}(D_{SC}^{ini})$	1 km			✓✓✓✓✓✓✓✓			
5 km				✓✓✓✓✓✓✓✓				
$C_i^{ini}$ -Depth-averaged volumetric frazil concentration in outflow	$0.2 \times 10^{-6}$			✓✓✓✓✓✓✓✓				
	$5 \times 10^{-6}$			✓✓✓✓✓✓✓✓				
	0			✓✓✓✓✓✓✓✓				
$V_a$ -Ambient flow speed	0			✓✓✓✓✓✓✓✓				
	$-0.02 \text{ m s}^{-1}$			✓✓✓✓✓✓✓✓				
$\bar{n}$ -Average number of frazil crystals in all size classes per unit volume	$200 \text{ m}^{-3}$			✓✓✓✓✓✓✓✓				
	$5000 \text{ m}^{-3}$			✓✓✓✓✓✓✓✓				
$D_{ini}(D_{SC}^{ini})(m)$ -Constant ISW plume outflow thickness (constant outflow supercooled layer thickness)	✓	✓	✓	✓	✓	✓	✓	✓
	30	50	65	70	78	95	100	110

77°55'14" S, 161°57'17" E



77°00'05" S, 168°41'10" E

Figure 1: Satellite image of McMurdo Sound region on 29 Nov. 2011. Purple and green frames outline the model and ice borehole (Fig. 6) domains, respectively. Colours within the purple frame indicate the steady state supercooled ISW plume thickness calculated by the vertically-modified ISW plume model in the standard run (Fig. 5d). Light gray lines outline McMurdo Ice Shelf front and coastlines. Model boundaries d-a, a-b (except the ISW outflow) and “b-c” are treated as solid walls, while “c-d” is an open boundary. Blue and red dots respectively mark the oceanographic CTD and ice drilling sites, and the blue arrow represents the location of the ISW outflow in the model. The red arrow in the inset (bottom-left) points to the location of the McMurdo Sound region. Location names C, I, W, NN, and FN mean Central, Intermediate, West, Near North, and Far North, respectively. Satellite image: NASA Rapid Response MODIS Subsets (<http://earthdata.nasa.gov/data/near-real-time-data/rapidresponse/modis-subsets>).



5 Figure 2: (a) Exponential profiles of equilibrium frazil concentration for selected values of  $Z^*$ . Coloured bars at the right and horizontal dashed lines indicate the distribution of supercooling (blue,  $T_{SC} > 0$ ) and overheating (red,  $T_{SC} < 0$ ) for the values of  $\sigma_{SC}$  used in (b). (b) Dependence of integral value of  $I_{gr}$  on  $Z^*$  for suspended frazil ice freezing ( $I_{gr} > 0$ ) and melting ( $I_{gr} < 0$ ) under the supercooling conditions shown in (a). The star denotes the particular conditions under which the integral values of  $I_{gr}$  calculated using VU and VM formulations are equal. Note that different y-axis scales are used for freezing and melting.

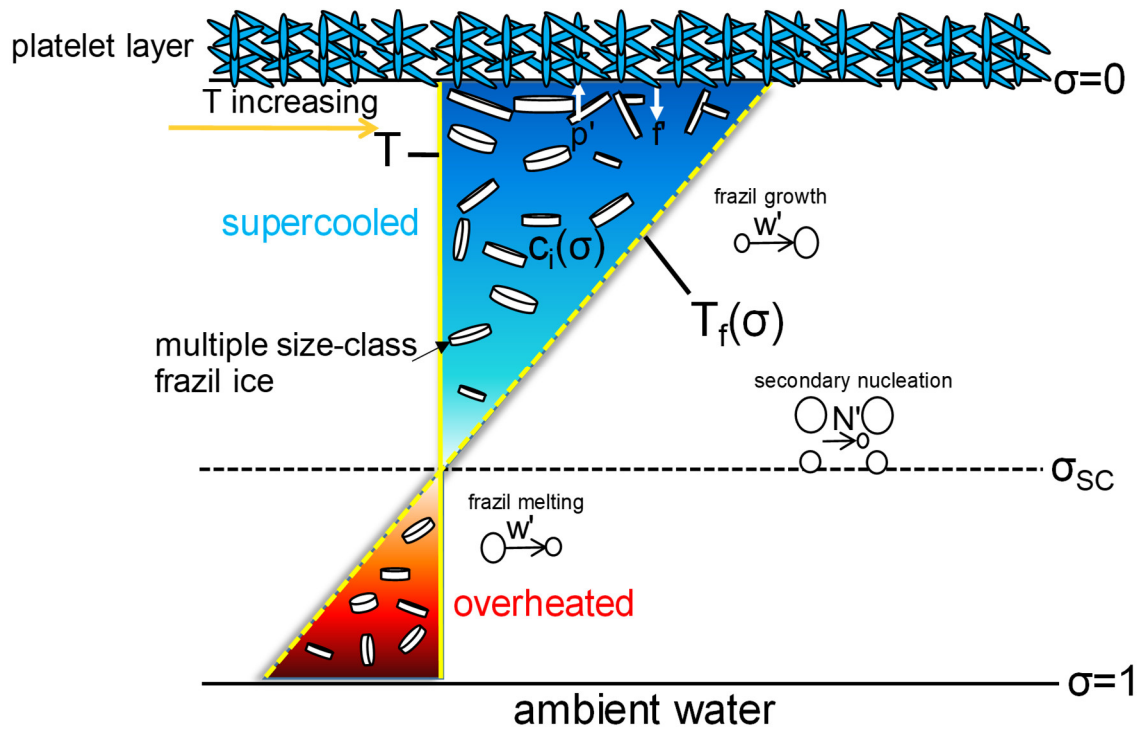


Figure 3: Schematic diagram of vertical distribution of thermal forcing and relevant processes within a supercooled ISW plume of homogeneous temperature and salinity. Secondary nucleation is the process by which the frazil ice in the smallest class is supplemented by collisions between other larger frazil ice crystals.



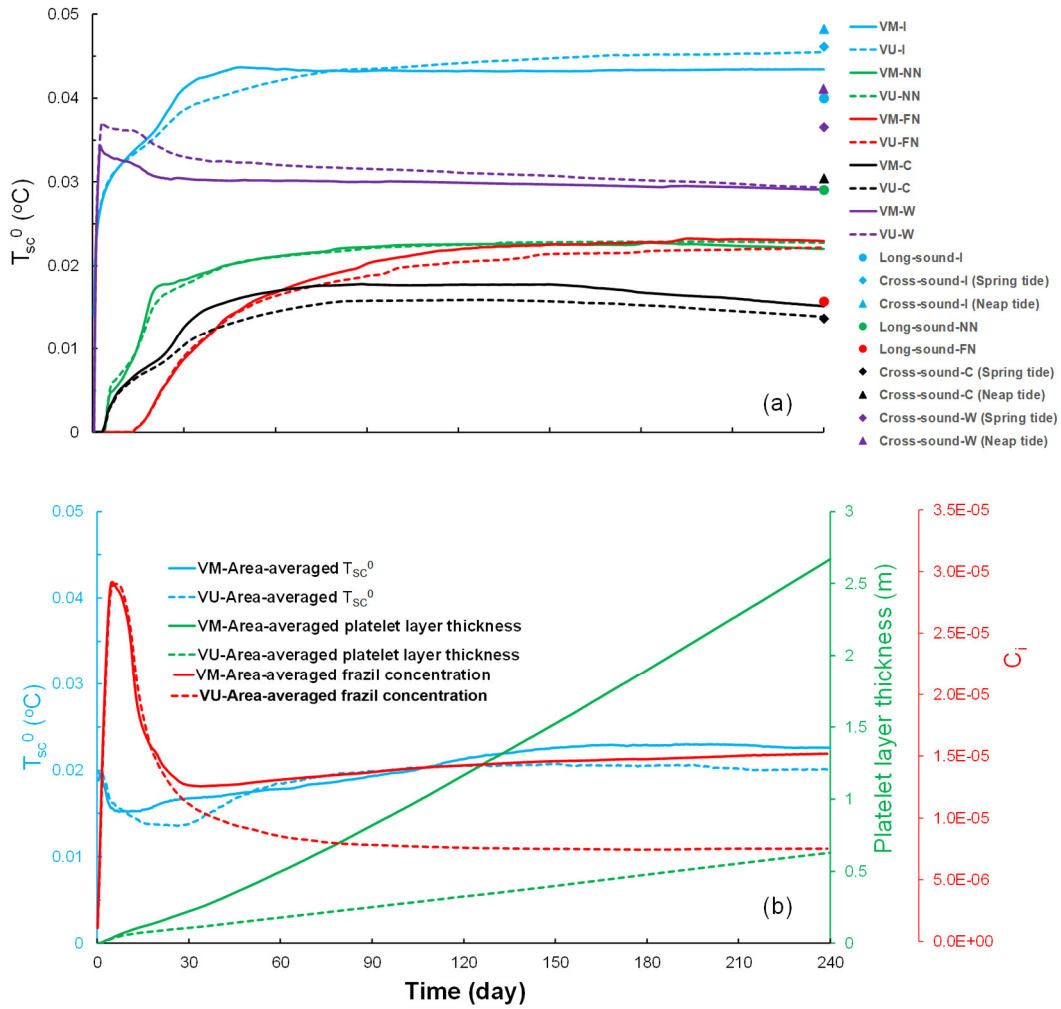


Figure 4: (a) Time series of  $T_{sc}^0$  simulated by VM (solid lines) and VU (dashed lines) models at five oceanographic sites (colour-coded) in the McMurdo Sound region. (b) Time series of area-averaged  $T_{sc}^0$  (blue), platelet layer thickness (green), and frazil concentration (red) simulated by VM (solid lines) and VU (dashed lines) models over the model domain (purple frame in Fig. 1).

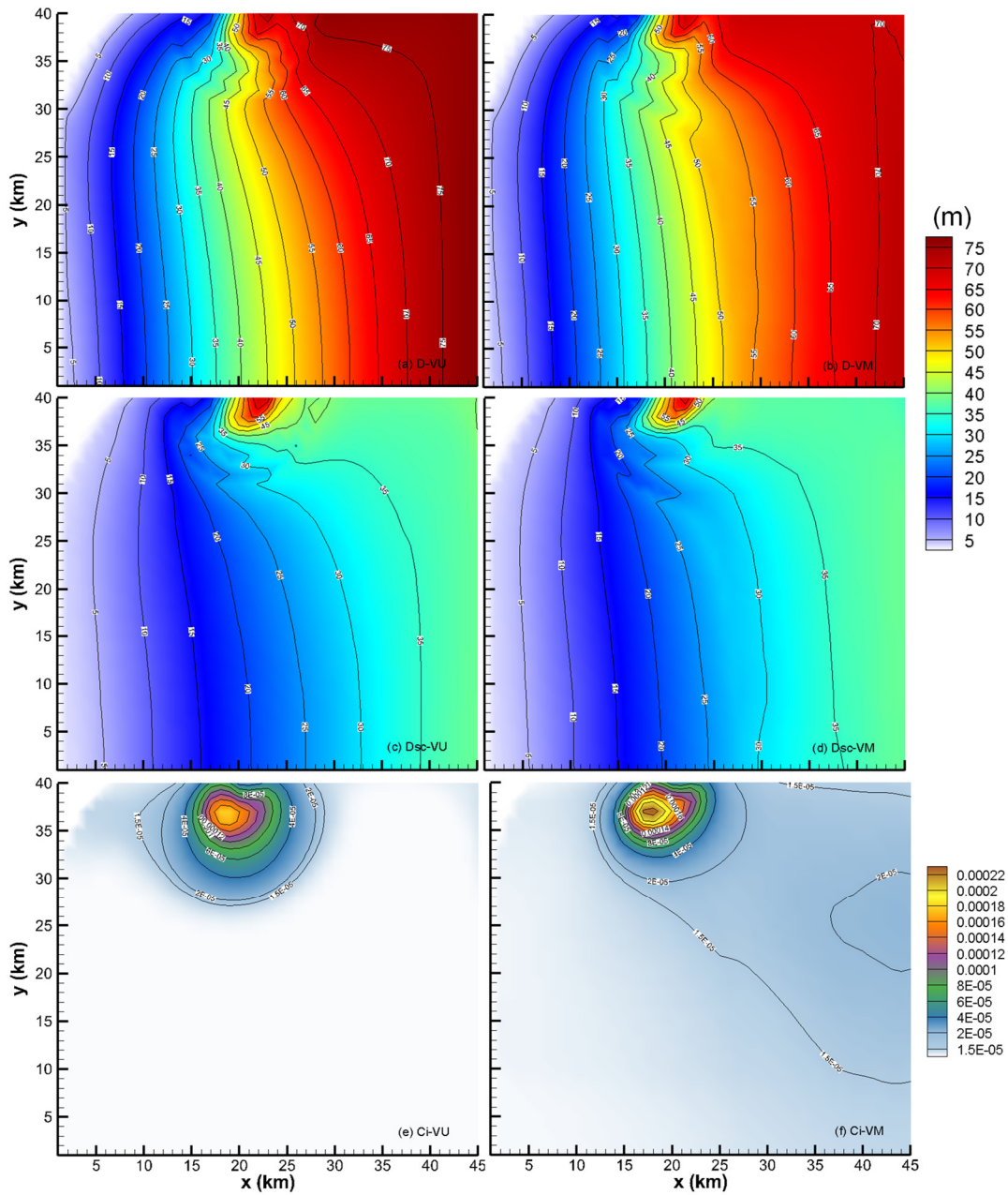


Figure 5: Spatial patterns, interpolated from model results using Natural Neighbour method, of (a), (b) total, (c), (d) supercooled ISW plume thickness, and (e), (f) depth-averaged frazil concentration at the end of the standard runs of (a), (c), (e) VU and (b), (d), (f) VM models over the domain (purple frame in Fig. 1). Note that the colour scale used in (a-d) is unified.

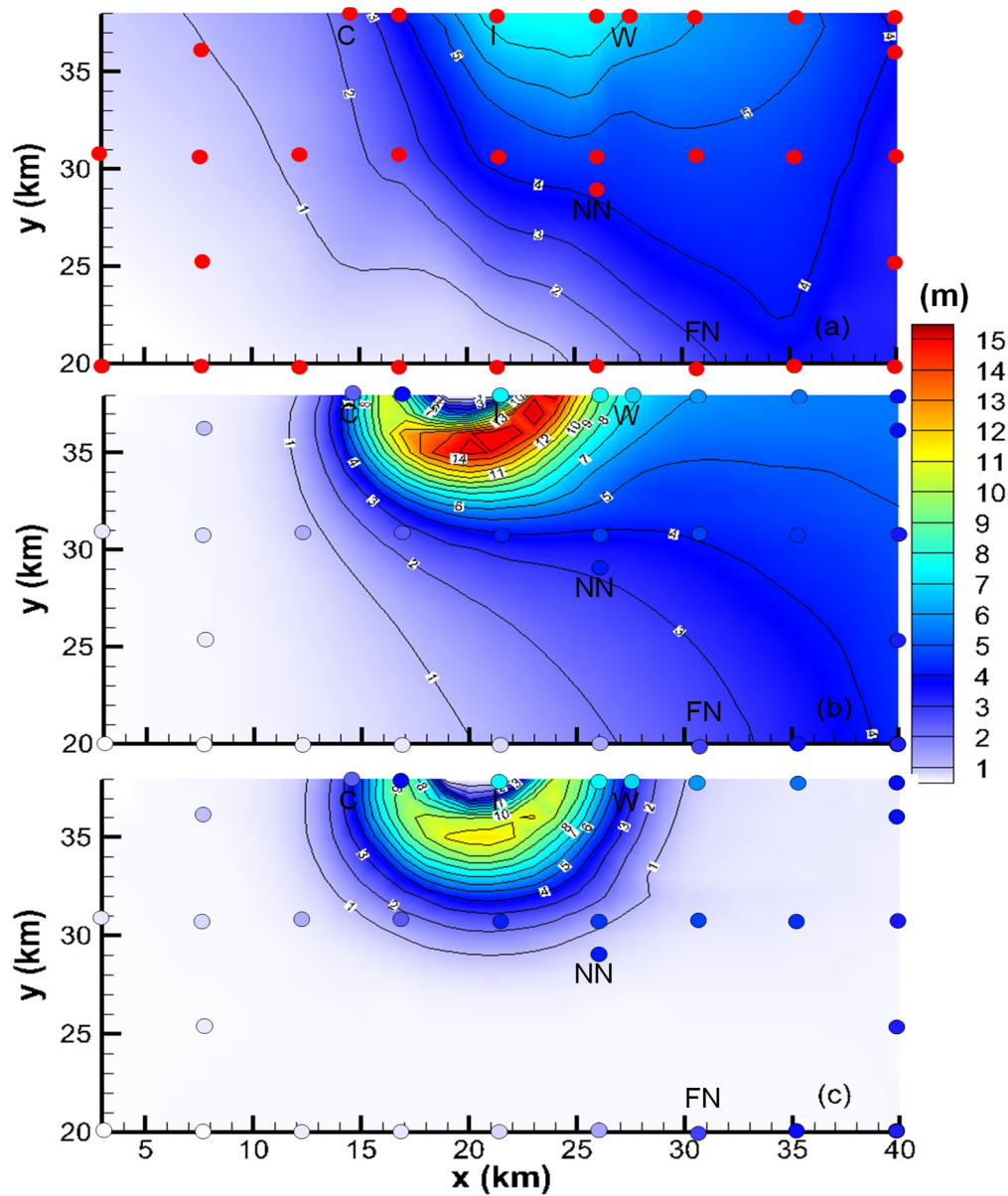


Figure 6: (a) Platelet layer thickness over green box in Fig. 1 interpolated, using Natural Neighbor method, from ice-core measurements (red dots). (b) and (c) platelet layer thickness derived from (b) VM and (c) VU models, compared with ice-core measurements (colour-coded dots). Note that the colour scale is unified.

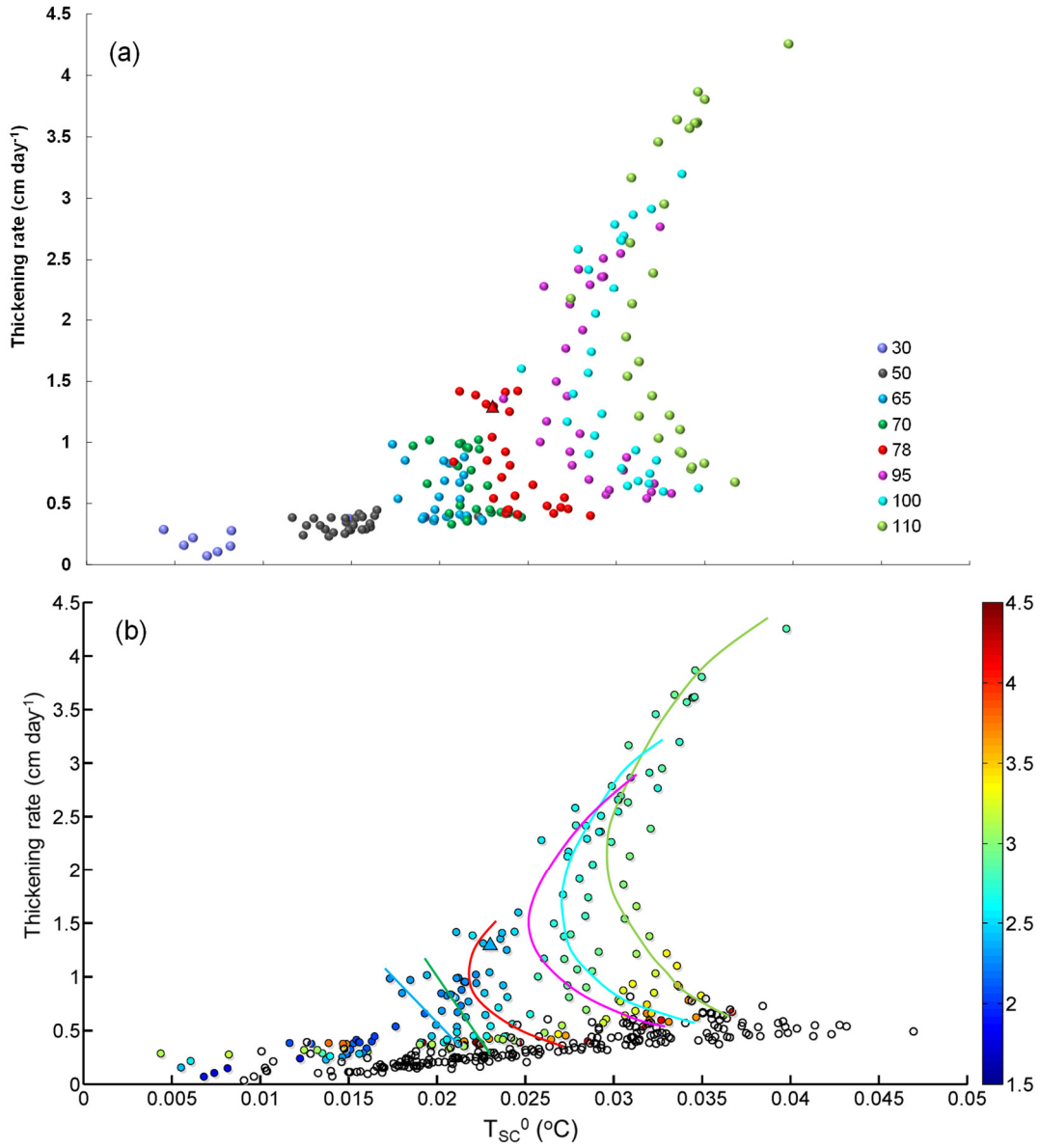


Figure 7: Relationship between  $T_{SC}^0$  and thickening rate classified by (a) outflow supercooled layer thickness  $D_{SC}^{ini}$  and (b)  $\bar{Z}_*$  (colour-coded). Numbers in legend of (a) represent the values of  $D_{SC}^{ini}$ . Solid and hollow dots in (b) correspond to the VM and VU model runs, respectively. Coloured lines depict the central trend of the corresponding data points shown in (a). Triangle corresponds to the standard run. The results are from the last 30 days of the model runs.

5

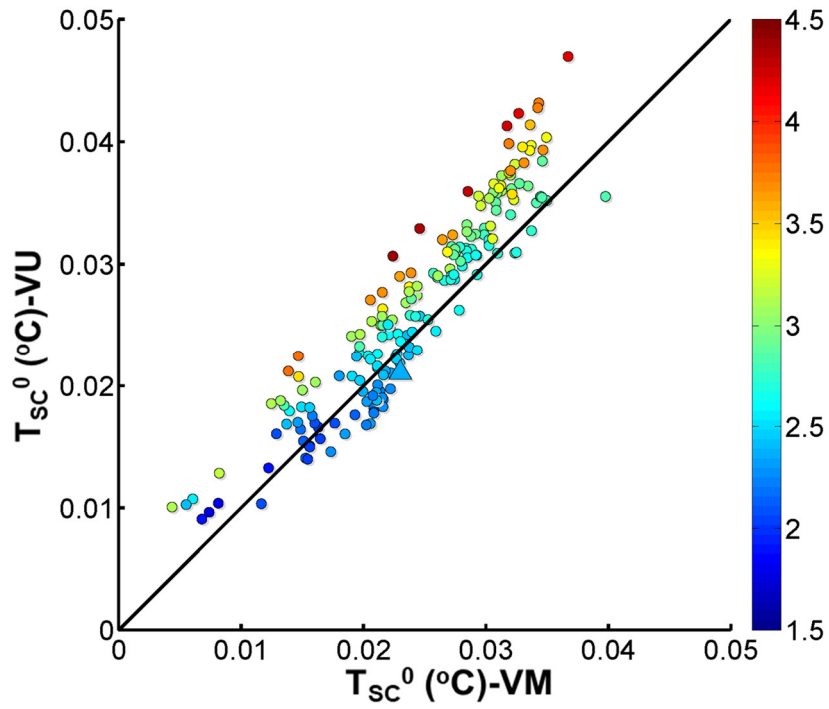


Figure 8: Comparison of  $T_{sc}^0$  calculated by the VM and VU models. Triangle corresponds to the standard run. The colour scale of  $\bar{Z}_*$  is the same as in Figure 7b.

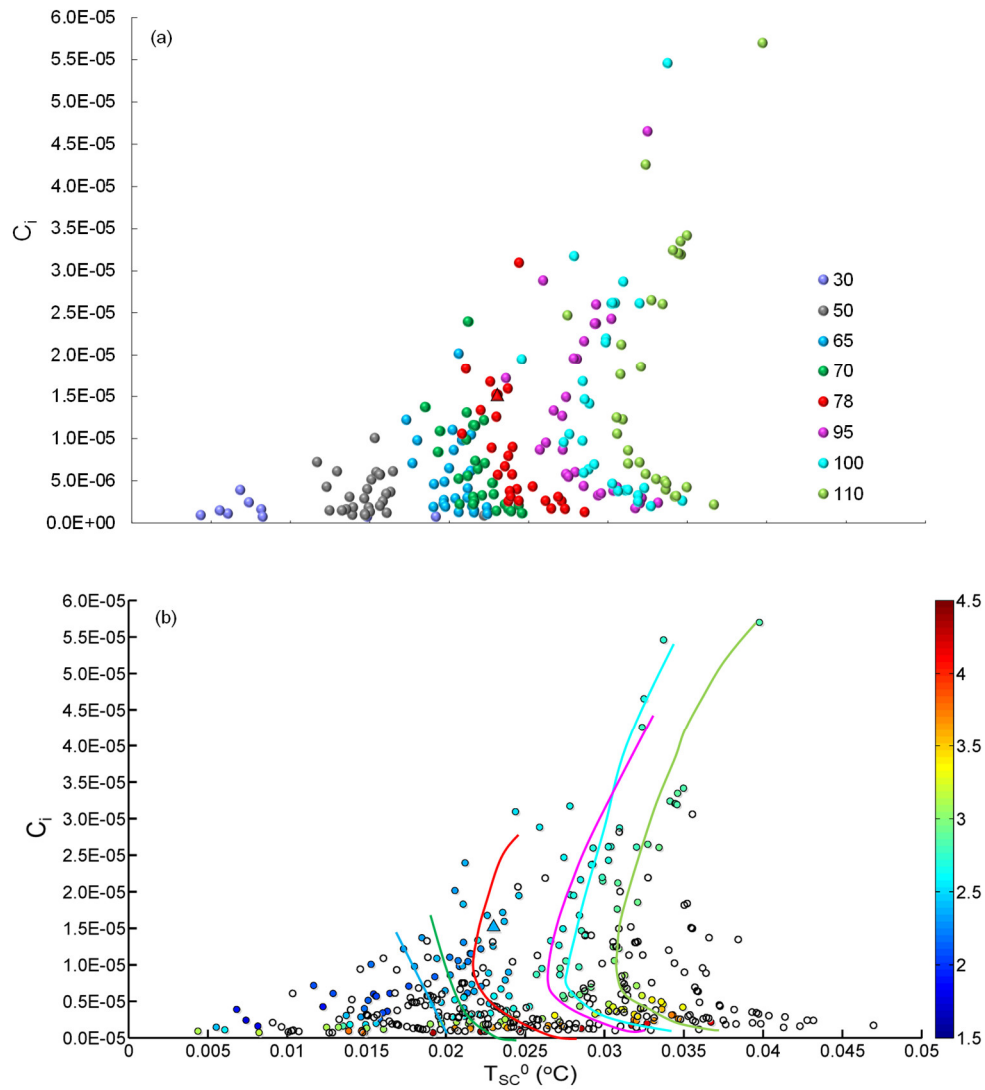
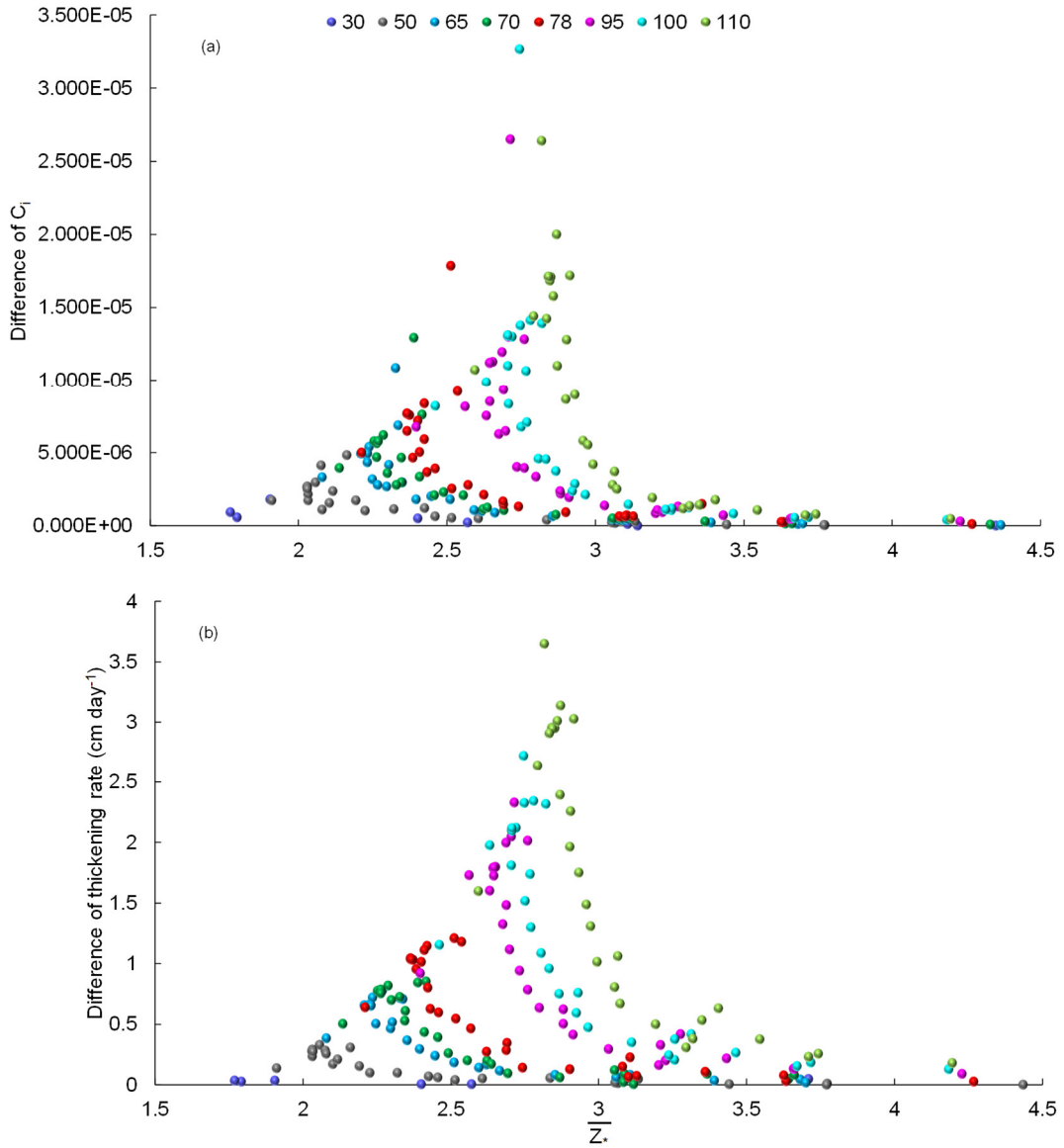


Figure 9: Same as Fig. 7, but for the relationship between  $T_{sc}^0$  and  $C_i$ .



**Figure 10: Relationship between  $\bar{Z}_*$  and difference of (a)  $C_i$  and (b) thickening rate calculated by VM and VU models (VM minus VU), classified by outflow supercooled layer thickness  $D_{SC}^{int}$ . Numbers in legend represent the values of  $D_{SC}^{int}$ .**